1521-009X/46/6/823–834$35.00
DRUG METABOLISM AND DISPOSITION

https://doi.org/10.1124/dmd.117.079673
Drug Metab Dispos 46:823–834, June 2018

Pharmacokinetics-Based Identification of Potential Therapeutic Phthalides from XueBiJing, a Chinese Herbal Injection Used in Sepsis Management[S]

Nating Zhang, Chen Cheng, Olajide E. Olaleye, Yan Sun,[1] Li Li, Yühong Huang, Feifei Du, Junling Yang, Fengqing Wang, Yanhong Shi, Fang Xu, Yanfen Li, Qi Wen,[2] Naixia Zhang, and Chuan Li

State Key Laboratory of Drug Research, Shanghai Institute of Materia Medica, Chinese Academy of Sciences, Shanghai (Nat.Z., C.C., O.E.O., Y.Su., L.L., F.D., J.Y., F.W., Y.Sh., F.X., Q.W., Nai.Z., C.L.); University of Chinese Academy of Sciences, Beijing (Nat.Z., C.L.); and Second Affiliated Hospital, Tianjin University of Traditional Chinese Medicine, Tianjin (Y.H., Y.L.), China

Received November 22, 2017; accepted March 7, 2018

ABSTRACT

XueBiJing, an injectable five-herb preparation, has been incorporated into routine sepsis care in China. Phthalides, originating from XueBiJing's component herbs *Ligusticum chuanxiong* rhizomes and *Angelica sinensis* roots, are believed to contribute to its therapeutic effects due to their presence in the preparation and antisepsis-related properties. This investigation aimed to identify potential therapeutic phthalides that are bioavailable to act on XueBiJing's therapeutic targets and that could serve as pharmacokinetic markers to supplement classic biomarkers for sepsis care. Among 10 phthalides detected in XueBiJing, senkyunolides I and G were the major circulating phthalides in human subjects, but their different pharmacokinetics might influence their contribution to XueBiJing's therapeutic action. Senkyunolide I exhibited a large distribution volume (1.32 l/kg) and was moderately bound in plasma (54% unbound), whereas senkyunolide G exhibited a small distribution volume (0.10 l/kg) and was extensively bound in plasma (3% unbound). Clearance of senkyunolide I from the systemic circulation was governed by UGT2B15-mediated hepatic glucuronidation; the resulting electrophilic glucuronides were conjugated with glutathione in the liver. Senkyunolide G was selectively bound to albumin (99%) in human plasma. To our knowledge, the human pharmacokinetic data of XueBiJing's phthalides are reported here for the first time. Based on this investigation and such investigations of the other component herbs, follow-up pharmacodynamic assessments of bioavailable herbal compounds are planned to elucidate XueBiJing's chemical basis responsible for its therapeutic action. Senkyunolides I and G, having the preceding disposition characteristics that could be detectably altered by septic pathophysiology, could serve as pharmacokinetic markers for sepsis care.

Introduction

Sepsis is life-threatening organ dysfunction caused by a dysregulated host response to infection (Singer et al., 2016). Current pharmacotherapy of sepsis relies on timely and appropriate antimicrobials and resuscitation therapies. Despite progress in understanding the pathophysiology of sepsis, the search for pharmacotherapies for modulating the septic response has been unsuccessful (Cohen et al., 2015).

XueBiJing, an intravenous preparation approved by the China Food and Drug Administration (China FDA) in 2004, has been incorporated into routine sepsis care (Chinese Society of Critical Care Medicine, 2015). In China, about 800,000 patients use XueBiJing each year, and 80% of them are patients with sepsis or septic shock. XueBiJing is prepared from a combination of *Carthamus tinctorius* flowers (Honghua in Chinese), *Paeonia lactiflora* roots (Chishao), *Ligusticum chuanxiong* rhizomes (Chuanxiong), *Angelica sinensis* roots (Danggui), and *Salvia miltiorrhiza* roots (Danshen). Many clinical studies in China have provided evidence that adding XueBiJing to the conventional management of sepsis reduces septic patients' 28-day mortality and incidence of complications, improves their Acute Physiology and Chronic Health Evaluation II scores and prognosis, and shortens their stay in intensive care units, with a low incidence of side effects (Chen and Li, 2013; Gao et al., 2015). A recent prospective, multicenter, randomized, single-blinded clinical trial in 710 patients with severe pneumonia showed that adding XueBiJing (100 ml twice a day for 5–7 days) to treatment could significantly reduce mortality (15.9% and 24.6% for the

This work was supported by the National Science and Technology Major Project of China "Key New Drug Creation and Manufacturing Program" [Grants 2009ZX09304-002, 2011ZX09201-201-23, 2017ZX09301012006]; the National Science Foundation of China for Distinguished Young Scholars [Grant 30925044]; the National Basic Research Program of China [Grant 2012CB518403]; the National Natural Science Foundation of China [Grant 81503345]; and the Strategic Priority Research Program of the Chinese Academy of Sciences [Grant XDA12050306].

This work was presented in part as a poster presentation at the following workshop: Zhang N-T et al. Systemic exposure to and disposition of phthalides from *Ligusticum chuanxiong* rhizomes and *Angelica sinensis* roots after intravenous administration of XueBiJing injection in human subjects and rats. *CPSA*; 2015 April 15–18; Shanghai, China.

[1]Current affiliation: Laboratory of Phase I Clinical Trials, Fudan University Shanghai Cancer Center, Shanghai, China.

[2]Visiting postgraduate from Hainan Medical University, Hainan, China.

https://doi.org/10.1124/dmd.117.079673.

[S]This article has supplemental material available at dmd.aspetjournals.org.

ABBREVIATIONS: $AUC_{0-\infty}$, area under concentration-time curve from 0 to infinity; $CL_{tot,p}$, total plasma clearance; f_u, unbound fraction of compound in plasma; GSH, glutathione; HLM, human liver microsomes; K_m, Michaelis constant; RLM, rat liver microsomes; TCM, traditional Chinese medicine; UGT, uridine 5′-diphosphoglucuronosyltransferase; V_{max}, maximum velocity; V_{SS}, apparent volume of distribution at steady state.

XueBiJing-treated and control groups, respectively) and increase the percentage of patients having improved pneumonia severity index (60.8% and 46.3%, respectively) (Song et al., 2016). XueBiJing was found to inhibit the uncontrolled release of inflammatory mediators, relieve an early overabundant innate immune response and potentially cumulative immunosuppression, attenuate crosstalk between inflammation and coagulation, protect endothelial cells, and maintain the physiologic functions of vital organs (Yin and Li, 2014; Liu et al., 2015; Dong et al., 2016). Unlike for most investigational antiseptic drugs developed from bench to bedside, research on XueBiJing proceeds from bedside to bench to bedside. Further research on this herbal medicine might facilitate a better understanding of pathophysiology of sepsis and the discovery of new antiseptic pharmacotherapies.

Despite the promising results of clinical studies, XueBiJing's chemical basis responsible for its therapeutic action is largely unknown; this impedes exploring how XueBiJing compounds and their synergistic interactions can affect sepsis. Such chemical basis comprises those constituents, of the herbal medicine, having sufficient bioavailability to and biopersistence at the sites of the medicine's therapeutic action after dosing and having intrinsic ability to produce the desired pharmacodynamic effects in their exposure forms, unchanged and/or metabolized. Here, the bioavailability means the amounts and ability of the medicine's constituents and/or their bioactive metabolites to pass through multiple biologic barriers in the body to access the action sites, while the biopersistence means the residence time of these compounds at the action sites for their pharmacodynamic effects to have therapeutically meaningful durations. Hence, multicompound pharmacokinetic research on XueBiJing has been proposed and the results will prioritize its compounds for pharmacodynamic assessments. Meanwhile, such research could also help identify those herbal compounds with detectably altered pharmacokinetics in response to sepsis as pharmacokinetic markers to reflect and predict abnormal cellular processes in tissues and treatment-caused reversion toward normal states. Based on their antisepsis-related properties and presence in XueBiJing, four types of compounds—i.e., Chuanxiong/Danggui phthalides, Honghua flavonoids, Chishao monoterpene glycosides, and Danshen catechols (Huang et al., 2011)—are being investigated in our ongoing serial pharmacokinetic research on the medicine (Cheng et al., 2016b; Li et al., 2016). As a part of this research, our current investigation focused on phthalides. Many phthalides, as pure isolates from Chuanxiong and Danggui, have shown antiinflammatory, antioxidant, and neuroprotective properties in cell- and animal-based studies (Qi et al., 2010; Or et al., 2011; Feng et al., 2012). The aim of this investigation was to identify potential therapeutic phthalides that are bioavailable to act on XueBiJing's therapeutic targets and that could serve as pharmacokinetic markers to supplement classic biomarkers for sepsis care. To our knowledge, the human pharmacokinetic data of phthalides in XueBiJing are reported here for the first time.

Materials and Methods

A detailed description of the materials and methods is provided in the Supplemental Materials and Methods, which is available online.

Drug Products, Chemicals, and Reagents

Samples of nine lots (1309271, 1309281, 1309291, 1309301, 1405301, 1406161, 1408191, 1410081, and 1501181) of XueBiJing with a China FDA drug ratification number of GuoYaoZhunZi-Z20040033 were obtained from Tianjin Chasesun Pharmaceuticals (Tianjin, China). Each milliliter of XueBiJing is prepared from a combination of 0.1 g each of Honghua (*C. tinctorius* flowers), Chishao (*P. lactiflora* roots), Chuanxiong (*L. chuanxiong* rhizomes), Danggui (*A. sinensis* roots), and Danshen (*S. miltiorrhiza* roots), yielding an herb-to-injection ratio of 1:2. The final product of XueBiJing is a sterile and nonpyrogenic dosage form for intravenous administration and is standardized to contain 1.0–1.7 mg/ml paeoniflorin and 0.2–0.5 mg/ml hydroxysafflor yellow A. Crude material samples of Chuanxiong (*L. chuanxiong* rhizomes) and Danggui (*A. sinensis* roots) were also obtained from Tianjin Chasesun Pharmaceuticals.

Senkyunolides A, G, H, I, and N, 3-*n*-butylenephthalide, 3-*n*-butylphthalide, 3-hydroxy-3-*n*-butylphthalide, levistolide A, and *Z*-ligustilide were obtained from Shanghai Yuanye Bio-Technology (Shanghai, China) or Shanghai Standard Technology (Shanghai, China); the compounds' purity was $\geq$ 98%. Pooled human liver microsomes (HLM), prepared from Chinese male and female human livers, were obtained from Research Institute for Liver Diseases (Shanghai, China), while pooled rat liver microsomes (RLM) were prepared from livers of male Sprague-Dawley rats in-house by differential centrifugation. The cDNA-expressed human uridine 5′-diphosphoglucuronosyltransferase (UGT) enzymes were obtained from Corning Gentest (Woburn, MA). Reduced glutathione (GSH), UDP-GlcUA, and human plasma γ-globulins were obtained from Sigma-Aldrich (St. Louis, MO). Human plasma albumin, α_1-acid glycoprotein, high-density lipoproteins, low-density lipoproteins, and very-low-density lipoproteins were obtained from Athens Research & Technology (Athens, GA). Chemical reagents and organic solvents were obtained from Sinopharm Chemical Reagent (Shanghai, China).

Human Pharmacokinetic Study of XueBiJing

A single-center, open-label human study of XueBiJing was performed at the National Clinical Research Center of the Second Affiliated Hospital of Tianjin University of Traditional Chinese Medicine (Tianjin, China). The study procedure was approved by an ethics committee of clinical investigation at the hospital and was performed in accordance with the Declaration of Helsinki. The study was registered at the Chinese Clinical Trials Registry (www.chictr.org) with a registration number of ChiCTR-ONRC-13003932. Healthy volunteers (18–35 years of age) were recruited and gave written informed consent forms to participate in the study.

Human subjects were randomly assigned to three groups (six male and six female in each group). The subjects received a single dose of one of the following the dosage regimens: 1) a single 1.25-hour infusion of a 100-ml preparation (diluted with 100 ml of 0.9% NaCl injection), 2) a single 2.5-hour infusion of a 100-ml preparation (diluted with 200 ml of 0.9% NaCl injection), or 3) a single 1.25-hour infusion of a 50-ml preparation (diluted with 100 ml of 0.9% NaCl injection). The test dosage regimens were designed according to the label dose of XueBiJing (100 ml/time per person) at an infusion rate that is commonly used for XueBiJing in clinics to treat patients with sepsis (regimen 1) and the label doses of XueBiJing (50 and 100 ml/time per person) at an infusion rate that is generally recommended for intravenous administration of Chinese herbal injections (regimens 2 and 3). Serial blood and urine samples were collected just before starting the infusion and, at intervals, up to 24 hours after starting the infusion (Supplemental Table 1). In addition, the six male subjects of regimen 3 continued to receive the same dose of XueBiJing each day for the following 6 days, and both blood and urine samples were collected (Supplemental Table 1). All blood samples were heparinized and centrifuged for plasma preparation.

Supportive Rat Pharmacokinetic Studies of XueBiJing

All animal care and experimental procedures complied with the *Guide for the Care and Use of Laboratory Animals* adopted and promulgated by the U.S. National Institutes of Health and were approved by the Institutional Animal Care and Use Committee at Shanghai Institute of Materia Medica (Shanghai, China). Male Sprague-Dawley rats (230–270 g, 6–8 weeks) were obtained from Sino-British SIPPR/BK Laboratory Animal (Shanghai, China). Some rats received femoral-artery-cannulation for blood sampling, and others underwent bile-duct-cannulation for bile sampling (Chen et al., 2013). A total of 62 rats were used in the experiments described here.

In the first study, 18 rats were randomly assigned to three groups (six rats in each group). The rats received a single 0.5-hour intravenous infusion of XueBiJing at 10, 30, or 90 ml/kg. The dosage of 10 ml/kg for rats was derived from the label dose of XueBiJing for patients (100 ml/time per person) according to dose normalization by body surface area (Reagan-Shaw et al., 2008). Serial blood samples were collected just before starting the infusion and, at intervals, up to 24 hours after starting the infusion. In the second study, six rats, housed individually in metabolic cages, received a single 0.5-hour intravenous infusion of

XueBiJing at 10 ml/kg, and urine and fecal samples were collected just before starting the infusion and, at intervals, up to 24 hours after starting the infusion. In the third study, six rats received a single 0.5-hour intravenous infusion of XueBiJing at 10 ml/kg, and bile samples were collected just before starting the infusion and, at intervals, up to 24 hours after starting the infusion. In the fourth study, 20 rats, under isoflurane anesthesia, were killed by bleeding from the abdominal aorta after an intravenous bolus dose of XueBiJing at 10 ml/kg. The lungs, heart, brain, kidneys, and liver were excised and homogenized, and the blood was also collected. In the fifth study, 12 rats were randomly assigned to two groups to receive a single 0.5-hour intravenous infusion of XueBiJing at 10 ml/kg (each milliliter of XueBiJing containing 0.3 μmol of senkyunolide I) or the injectable solution of purified senkyunolide I at 3.0 μmol/kg. Serial blood samples were collected just before starting the infusion and, at intervals, up to 24 hours after starting the infusion. All blood samples were heparinized and centrifuged for plasma preparation.

Supportive In Vitro Characterizations of Phthalides

Metabolism Studies. In vitro metabolism studies were performed to characterize tentative XueBiJing phthalide metabolites that had been detected in vivo. Because of detection of glucuronides of XueBiJing phthalides in excretory samples of human subjects and rats receiving XueBiJing, senkyunolides I, G, H and N, and 3-hydroxy-3-*n*-butylphthalide were incubated with UDP-GlcUA-fortified HLM or UDP-GlcUA-fortified RLM to glucuronidate these phthalides, and the incubation conditions were as described by Hu et al. (2013). The in vitro glucuronidation of senkyunolide I was repeated with addition of GSH into the incubation. In addition, senkyunolide I was incubated directly with GSH. The cDNA-expressed human UGTs were used to identify which human UGT isoforms could mediate glucuronidation of senkyunolide I. UGT1A9, UGT2B15, UGT2B17, HLM, and RLM were compared with respect to their metabolic capability for mediating the glucuronidation of senkyunolide I.

Assessment of Protein Binding (Total Plasma and Individual Proteins). Unbound fraction in plasma (f_u) was assessed for senkyunolides I, G, H, and N, and 3-hydroxy-3-*n*-butylphthalide by a method of rapid ultrafiltration (at 13,362*g* and 37°C for 3 minutes) described by Guo et al. (2006). This method was also used to identify the proteins responsible for binding senkyunolides I and G in human plasma by individually spiking the test compounds into solutions of isolated test proteins at their physiologic concentrations (Urien et al., 1992).

Caco-2 Cell-Based Assessment of Membrane Permeation Rate. To help understand their in vivo reach, the rate of membrane permeation of senkyunolides I, G, H, and N, and 3-hydroxy-3-*n*-butylphthalide was assessed using Caco-2 cell monolayers under "sink" conditions (Dai et al., 2008).

Assessment of Blood-Plasma Partition. Blood-to-plasma concentration ratios were determined for senkyunolides I and G in human and for senkyunolides I, G, H, and N, and 3-hydroxy-3-*n*-butylphthalide in rats using a method described by Chen et al. (2013).

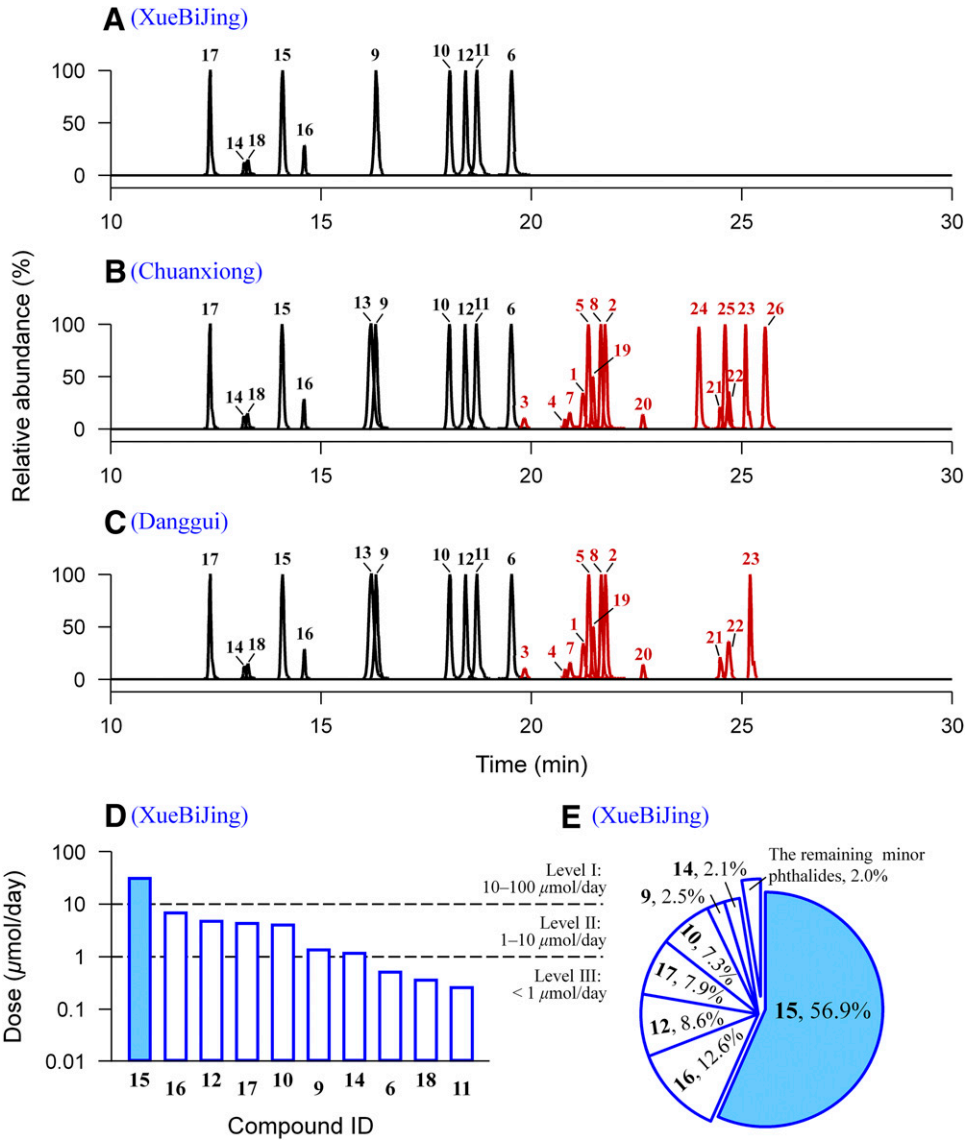

Fig. 1. Phthalides detected in XueBiJing. (A) Stacked chromatogram of phthalides, detected by mass spectrometry, in XueBiJing. (B and C) Stacked chromatograms of phthalides, detected by mass spectrometry, in XueBiJing's component herbs Chuanxiong (*L. chuanxiong* rhizomes) and Danggui (*A. sinensis* roots), respectively. (D) Mean doses of phthalides from nine lots of XueBiJing at 100 ml/day. (E) Percentage daily doses of phthalides in the total daily dose of phthalides from XueBiJing. See Table 1 for the compounds' names.

Preparation of Glucuronides of Senkyunolide I and Their Structural Elucidation by NMR

The glucuronides of senkyunolide I were biosynthesized by incubating isolated senkyunolide I with UDP-GlcUA-fortified RLM and were purified by liquid chromatography. The purified compounds were analyzed by NMR spectrometry using a Bruker AVANCE III-500 MHz spectrometer (Bremen, Germany) to elucidate their structures.

Detection and Characterization of Unchanged and Metabolized Phthalides

A Waters Synapt G2 high definition time-of-flight mass spectrometer (Manchester, United Kingdom), interfaced via a Zspray/LockSpray electrospray ionization source with a Waters Acquity UPLC separation module (Milford, MA), was used to analyze phthalides in samples of XueBiJing, pulverized Chuanxiong, and pulverized Danggui and to analyze unchanged and metabolized phthalides in samples obtained from human, rat, and in vitro studies. To facilitate these analyses, pre-analysis literature mining was conducted on phthalides of Chuanxiong and/or Danggui origin with respect to their names, chemical structures, presence in raw materials of Chuanxiong and Danggui and in Chinese medicines containing these herbs, pharmaceutical processing-related chemotransformation, liquid chromatography/mass spectrometry-based analyses, pharmacokinetics and metabolism, antisepsis-related properties, and toxicities. In addition, the detection of metabolized phthalides in samples from human and rat studies was also facilitated by the Accelrys metabolite database (version 2015.1; San Diego, CA), which was used to predict possible metabolic pathways of phthalides (Williams et al., 2012).

Quantification of Phthalides

An AB Sciex API 4000 Q Trap mass spectrometer (Toronto, Canada), interfaced via a Turbo V ion source with a Waters Acquity UPLC separation module, was used to quantify phthalides and related compounds in samples of different types. Matrix-matched calibration curves of senkyunolides I, H, G, and N, 3-hydroxy-3-*n*-butylphthalide, and senkyunolide I-7-*O*-β-glucuronide were constructed using weighted ($1/X$ or $1/X^2$) linear regression of the peak areas (Y) of the analytes against the corresponding nominal analytes' concentrations (X; 6, 19, 56, 167, 500, 1500, and 4500 nM), and the curves showed good linearity ($r^2 >$ 0.99). Sample preparation was performed using methanol-based treatment at a volumetric methanol-to-sample ratio of 3:1 for samples of human and rat studies and at a ratio of 1:1 for samples of in vitro metabolism studies.

The quantification method was validated according to the European Medicines Agency Guideline on Bioanalytical Method Validation (2012) to demonstrate their reliability and reproducibility for the intended use. The assays' lower limits of quantification were 19–56 nM for the analytes, and the upper limits of quantification were 4500 nM. The intrabatch accuracy and precision were 86%–112% and 2%–15%, respectively, and the interbatch values were 95%–113% and 3%–12%, respectively. The coefficients of variation of matrix factors were 1.3%–13.6%, which were within the required range (i.e., ≤15%). The stability of analytes under conditions mimicking the analytical process was evaluated: after storage at 24°C for 5 hours, after storage at 8°C for 24 hours, and after three freeze-and-thaw cycles. The test compounds were stable under the test conditions because the results (i.e., −15% to 9%) met the acceptance criterion (the measured mean concentration being within ±15% of the nominal concentration).

Data Analysis

Pharmacokinetic parameters were estimated by a noncompartmental method using the Thermo Scientific Kinetica 5.0 software package (version 5.0; Philadelphia, PA). The Michaelis constant (K_m) and maximum velocity (V_{max}) were estimated using GraphPad Prism software (version 5.01; San Diego, CA). The dose proportionality of senkyunolide I in the rats was assessed using the regression of log-transformed data (the Power model), with the criteria calculated according to the method described by Smith et al. (2000). Statistical analysis was performed using IBM SPSS Statistics software (version 19.0; Somers, NY). All data are expressed as the mean ± S.D. $P < 0.05$ was considered the minimum level of statistical significance.

Results

Phthalides Detected in XueBiJing and Their Relative Abundance. As the first step in the pharmacokinetic investigation of phthalides after dosing XueBiJing, an analysis of the chemical composition of phthalides in the medicine was performed to understand which and how much phthalides were introduced into the bloodstream via dosing. A total of 10 phthalides (Log*P*, 0.8–3.0) were detected in XueBiJing (Fig. 1; Table 1). More lipophilic phthalides (Log*P*, 3.0–5.0), including *Z*-ligustilide (**5**) (the most abundant phthalide in the raw herb materials Chuanxiong [*L. chuanxiong* rhizomes] and Danggui [*A. sinensis* roots]), were not detected in the preparation.

The detected phthalides were ranked according to their dose levels from XueBiJing at a label dose of 100 ml. After ranking, the detected phthalides were graded as level I (10–100 μmol/day), comprising senkyunolide I (**15**) (29.3 μmol/day); level II (1–10 μmol/day), comprising senkyunolides H (**16**), G (**12**), and N (**17**), 3-hydroxy-3-*n*-butylphthalide (**10**), *Z*-6,7-epoxyligustilide (**9**), and 6,7-dihydroxyligustilide (**14**) (1.1–6.5 μmol/day); and level III (<1 μmol/day), comprising the remaining phthalides (0.2–0.5 μmol/day). The dose of the level I phthalide, the sum of the doses of the level II phthalides, and the sum of the doses of the level III phthalides accounted for 56.9%, 41.0%, and

TABLE 1

Phthalides detected in samples of nine lots of XueBiJing

The nine lots of samples of XueBiJing were 1309271, 1309281, 1309291, 1309301, 1405301, 1406161, 1408191, 1410081, and 1501181. The details of detection, characterization, and quantification of phthalides in XueBiJing are described in the Supplemental Materials and Methods (Detection and Characterization of Unchanged and Metabolized Phthalides and Quantification of Phthalides). The dose level data represent the mean ± S.D. for samples of nine lots of XueBiJing.

ID	Compound	LC/TOF-MS^E Data			Molecular Mass	Molecular Formula	Log*P*	Dose Level	Lot-to-Lot Variability (RSD, %)
		t_R	Sodiated Molecule	Collision-Induced Fragmentation Profile					
		min	*m/z*	*m/z*	*Da*			*μmol/day*	
15	Senkyunolide I	14.07	247.0946	207.1021,[a] 189.0919, 161.0968	224.1049	$C_{12}H_{16}O_4$	0.8	29.31 ± 2.81	9.6
16	Senkyunolide H	14.61	247.0944	207.1019,[a] 189.0916, 161.0968	224.1049	$C_{12}H_{16}O_4$	0.8	6.48 ± 0.63	9.7
12	Senkyunolide G	18.44	231.1005	191.1072,[a] 149.0610, 135.0445	208.1099	$C_{12}H_{16}O_3$	1.5	4.45 ± 0.31	6.9
17	Senkyunolide N	12.36	249.1111	191.1064, 163.1116, 149.0602[a]	226.1205	$C_{12}H_{18}O_4$	1.2	4.08 ± 0.52	12.7
10	3-Hydroxy-3-*n*-butylphthalide	18.06	229.0846	189.0920, 171.0814, 133.0295[a]	206.0943	$C_{12}H_{14}O_3$	2.3	3.76 ± 0.48	12.6
9	*Z*-6,7-epoxyligustilide	16.30	229.0840	189.0907,[a] 161.0972, 143.0867	206.0943	$C_{12}H_{14}O_3$	1.7	1.27 ± 0.05	4.0
14	6,7-Dihydroxyligustilide	13.24	247.0939	207.1029, 189.0916, 161.0972[a]	224.1049	$C_{12}H_{16}O_4$	0.8	1.09 ± 0.11	10.2
6	Senkyunolide A	19.53	215.1053	193.1233,[a] 175.1128, 147.1178	192.1150	$C_{12}H_{16}O_2$	3.0	0.48 ± 0.26	54.0
18	Senkyunolide J	13.27	249.1094	191.1069, 163.1124, 153.0554[a]	226.1205	$C_{12}H_{18}O_4$	1.2	0.34 ± 0.04	12.7
11	4-Hydroxy-3-*n*-butylphthalide	18.72	229.0835	161.0972, 151.0392[a]	206.0943	$C_{12}H_{14}O_3$	2.7	0.24 ± 0.03	12.6

LC/TOF-MS, liquid chromatography/time-of-flight mass spectrometry; Log*P*, octanol-water partition coefficient; RSD, relative standard deviation; t_R, retention time.
[a]Product ion of base peak.

2.0% of the total dose of the phthalides in the preparation, respectively. XueBiJing exhibited lot-to-lot variability of 9.6% for the level I phthalide **15**, 4.0%–12.7% for level II phthalides, and 12.6%–54.0% for level III phthalides (Table 1). These data suggested that XueBiJing exhibited good quality consistency with respect to individual doses of its major phthalides.

Systemic Exposure to Phthalides in Human Subjects and Rats after Dosing XueBiJing. In human subjects, five unchanged phthalides were detected in plasma after starting an intravenous infusion of XueBiJing; they were not detected before dosing (Fig. 2; Supplemental Table 2). Senkyunolides I (**15**) and G (**12**) exhibited notably higher levels of systemic exposure than the other detected phthalides senkyunolide H (**16**), senkyunolide N (**17**), and 3-hydroxy-3-*n*-butylphthalide (**10**). These circulating phthalides, except phthalide **12**, were also detected in urine after dosing, with fractions of dose excreted ($f_{e\text{-}U}$) of 3.0%–18.3%. Chemical structures of these circulating phthalides are also shown in Fig. 2.

In rats, senkyunolides I (**15**), H (**16**), G (**12**), and N (**17**), and 3-hydroxy-3-*n*-butylphthalide (**10**) were detected in plasma after dosing XueBiJing (Fig. 2; Supplemental Table 2). However, unlike in human subjects, phthalide **12** exhibited a significantly lower exposure level in rats, relative to phthalide **15**. These circulating phthalides were also detected in urine except for phthalide **12**, and in bile except for phthalides **12** and **10** (Fig. 2). Their $f_{e\text{-}U}$ and fractions of dose excreted into bile ($f_{e\text{-}B}$) were 0.6%–2.8% and 0.2%–3.7%, respectively. Trace amounts of these phthalides were detected in rat feces.

The preceding excretory data suggested that the circulating phthalides were cleared mainly via metabolism. However, no circulating metabolites of phthalides were detected in human subjects or rats after dosing XueBiJing. Several metabolites of senkyunolides I (**15**) and G (**12**) were detected in excretory samples (Supplemental Tables 3 and 4), but metabolites of the other circulating phthalides were negligible or not detected. For phthalide **15**, its glucuronides ($\mathbf{M15_{G\text{-}1}}$ and $\mathbf{M15_{G\text{-}2}}$), dehydrated glutathione conjugates ($\mathbf{M15_{GSH\text{-}1}}$ and $\mathbf{M15_{GSH\text{-}2}}$), and degradation products of the glutathione conjugates (the cysteinylglycine conjugates $\mathbf{M15_{Cys\text{-}Gly\text{-}1}}$ and $\mathbf{M15_{Cys\text{-}Gly\text{-}2}}$ and the cysteine conjugates $\mathbf{M15_{Cys\text{-}1}}$ and $\mathbf{M15_{Cys\text{-}2}}$) were detected in rat bile. $\mathbf{M15_{G\text{-}1}}$, $\mathbf{M15_{G\text{-}2}}$, and *N*-acetylcysteine conjugates ($\mathbf{M15_{NAC\text{-}1}}$ and $\mathbf{M15_{NAC\text{-}2}}$) were detected in rat urine. $\mathbf{M15_{G\text{-}1}}$, $\mathbf{M15_{G\text{-}2}}$, $\mathbf{M15_{Cys\text{-}1}}$, and $\mathbf{M15_{Cys\text{-}2}}$ were detected in human urine. For phthalide **12**, its glucuronide ($\mathbf{M12_G}$) was detected in rat bile and urine, but not in human urine.

In Vitro Metabolism of Phthalides. Additional in vitro metabolism studies were performed to better understand the in vivo elimination of the circulating XueBiJing phthalides, and the results are shown in Table 2 and Figs. 3–5. Incubation of senkyunolide I with UDP-GlcUA-fortified HLM led to the formation of the glucuronides $\mathbf{M15_{G\text{-}1}}$ and $\mathbf{M15_{G\text{-}2}}$, with an $\mathbf{M15_{G\text{-}2}}$-to-$\mathbf{M15_{G\text{-}1}}$ peak area ratio of 66; the ratio for RLM was 5. $\mathbf{M15_{G\text{-}1}}$ and $\mathbf{M15_{G\text{-}2}}$ were characterized as senkyunolide

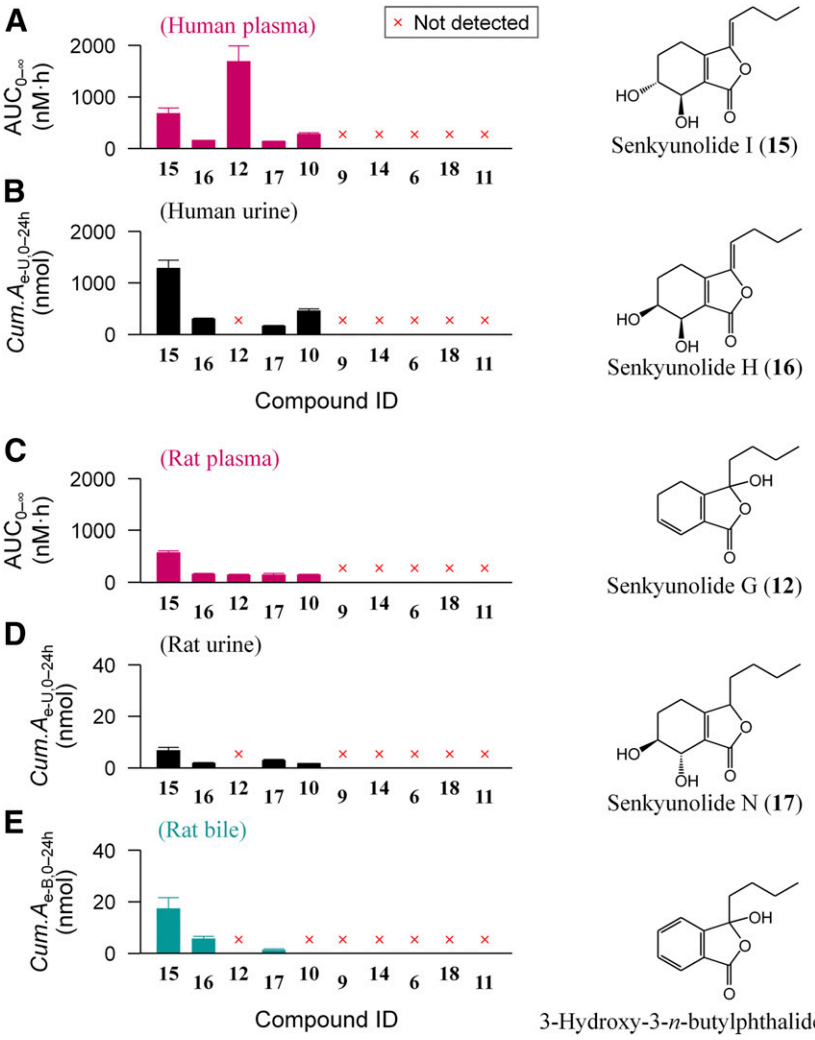

Fig. 2. Circulating phthalides from human subjects (n = 12) and rats (n = 6) that intravenously received XueBiJing and their chemical structures. Human plasma (A) and urine data (B) of XueBiJing, 1.25-hour infusion at 100 ml per subject. Rat plasma (C), urine (D), and bile data (E) of XueBiJing, 0.5-hour infusion at 10 ml/kg. (A–E) XueBiJing phthalides (shown as compound ID) are ranked in the same order as they are ranked in Fig. 1D (mean doses of phthalides from nine lots of XueBiJing at 100 ml/day). $Cum.A_{e\text{-}B\ 0\text{–}24\ h}$, cumulative amount excreted into bile from 0 to 24 hours; $Cum.A_{e\text{-}U\ 0\text{–}24\ h}$, cumulative amount excreted into urine from 0 to 24 hours.

TABLE 2

In vitro metabolism of senkyunolides I and G

The details of in vitro metabolism studies of senkyunolides I and G are described in the Supplemental Materials and Methods (Metabolism Studies).

Subcellular Fraction	Cofactor	Metabolite ID[a]	LC/TOF-MS^E Data			Molecular Mass	Molecular Formula	Presence in In Vivo Sample
			t_R	Ionized Molecule	Diagnostic FI or NL			
			min	*m/z*	*m/z or Da*	*Da*		
Substrate: senkyunolide I								
Rat liver microsomes	UDP-GlcUA	**M15$_{G-1}$**	12.71	$[M + Na]^+$/423.1259	NL, 176.0317	400.1369	$C_{18}H_{24}O_{10}$	Rat bile and urine
		M15$_{G-2}$	13.40	$[M + Na]^+$/423.1268	NL, 176.0321			Rat bile and urine
	UDP-GlcUA + GSH	**M15$_{G-1}$**	12.73	$[M + Na]^+$/423.1266	NL, 176.0323			Rat bile and urine
		M15$_{G-2}$	13.40	$[M + Na]^+$/423.1266	NL, 176.0323			Rat bile and urine
		M15$_{GSH-1}$	14.70	$[M + H]^+$/514.1844	NL, 129.0425	513.1781	$C_{22}H_{31}N_3O_9S$	Rat bile
				$[M - H]^-$/512.1703	FI, 272.0886			
		M15$_{GSH-2}$	15.67	$[M + H]^+$/514.1857	NL, 129.0428			Rat bile
				$[M - H]^-$/512.1702	FI, 272.0882			
Human liver microsomes	UDP-GlcUA	**M15$_{G-1}$**	12.72	$[M + Na]^+$/423.1264	NL, 176.0318	400.1369	$C_{18}H_{24}O_{10}$	Human urine
		M15$_{G-2}$	13.38	$[M + Na]^+$/423.1267	NL, 176.0321			Human urine
	UDP-GlcUA + GSH	**M15$_{G-1}$**	12.72	$[M + Na]^+$/423.1252	NL, 176.0323			Human urine
		M15$_{G-2}$	13.40	$[M + Na]^+$/423.1268	NL, 176.0324			Human urine
		M15$_{GSH-1}$	14.71	$[M + H]^+$/514.1846	NL, 129.0422	513.1781	$C_{22}H_{31}N_3O_9S$	ND in human samples
				$[M - H]^-$/512.1700	FI, 272.0883			
		M15$_{GSH-2}$	15.67	$[M + H]^+$/514.1860	NL, 129.0428			ND in human samples
				$[M - H]^-$/512.1703	FI, 272.0883			
Substrate: senkyunolide G								
Rat liver microsomes	UDP-GlcUA	**M12$_G$**	16.63	$[M + Na]^+$/407.1319	NL, 176.0319	384.1420	$C_{18}H_{24}O_9$	Rat bile and urine

FI, fragment ion; LC/TOF-MS, liquid chromatography/time-of-flight mass spectrometry; ND, not detected; NL, neutral loss; t_R, retention time.

[a]Metabolite ID provides information regarding parent compound, metabolite type, and metabolite isomer. For instance, M15 in **M15$_{G-1}$** denotes that the compound is a metabolite of senkyunolide I (**15**). The subscript letter G denotes glucuronide, and the subscript number 1 denotes the first eluted metabolite isomer. The subscript letter GSH denotes dehydrated glutathione conjugate. **M12$_G$** indicates that only one senkyunolide G glucuronide was detected.

I-6-*O*-*β*-glucuronide and senkyunolide I-7-*O*-*β*-glucuronide, respectively, using NMR data (Supplemental Table 5). Notably, senkyunolide I was found to be primarily glucuronized by human UGT2B15, with UGT1A9 and UGT2B17 playing a minor role (Fig. 3). Glucuronidation of senkyunolide I into senkyunolide I-7-*O*-*β*-glucuronide was saturable, with K_m, V_{max}, and intrinsic clearance of 18.4 ± 1.0 μM, 291 ± 5 pmol/min per milligram protein, and 15.8 μl/min per milligram protein, respectively, for cDNA-expressed human UGT2B15; 34.7 ± 3.2 μM, 7360 ± 254 pmol/min per milligram protein, and 212 μl/min per milligram protein, respectively, for HLM; and 185 ± 5 μM, 12305 ± 122 pmol/min per milligram protein, and 66.5 μl/min per milligram protein, respectively, for RLM. Another important finding was the electrophilicity of the glucuronides of senkyunolide I. As shown in Fig. 4, dehydrated GSH conjugates of senkyunolide I (**M15$_{GSH-1}$** and **M15$_{GSH-2}$**) were formed by GSH replacement of glucuronic acid in a second metabolic reaction. No GSH conjugates were detected after incubation of senkyunolide I directly with GSH. Both the in vivo metabolite profiling and the in vitro metabolism study suggested that the glucuronidation governed clearance of senkyunolide I (**15**) from the systemic circulation.

Glucuronidation of senkyunolide G occurred by incubation of this phthalide with UDP-GlcUA-fortified RLM and UDP-GlcUA-fortified HLM, but the formation rate of the glucuronide (**M$_{12G}$**) was quite slow in the latter. Glucuronides of senkyunolide H, senkyunolide N, and

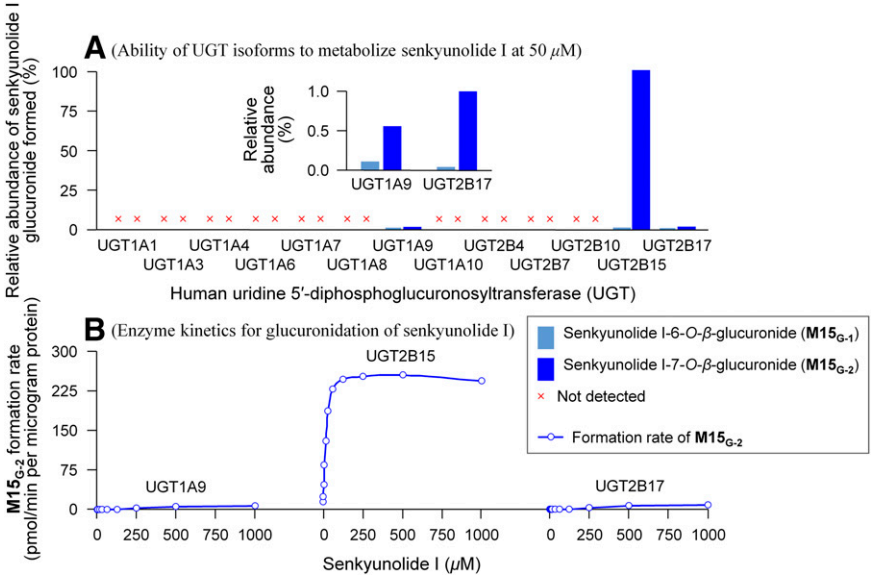

Fig. 3. High selectivity of senkyunolide I for human UGT2B15. (A) Glucuronidation activities of cDNA-expressed human UGT isoforms on senkyunolide I (50 μM). Senkyunolide I-7-*O*-*β*-glucuronide (**M15$_{G-2}$**) was preferentially formed, and senkyunolide I-6-*O*-*β*-glucuronide (**M15$_{G-1}$**) was a minor metabolite. (B) Comparative metabolic capabilities of human UGT1A9, UGT2B15, and UGT2B17 in mediating the glucuronidation of senkyunolide I into **M15$_{G-2}$**.

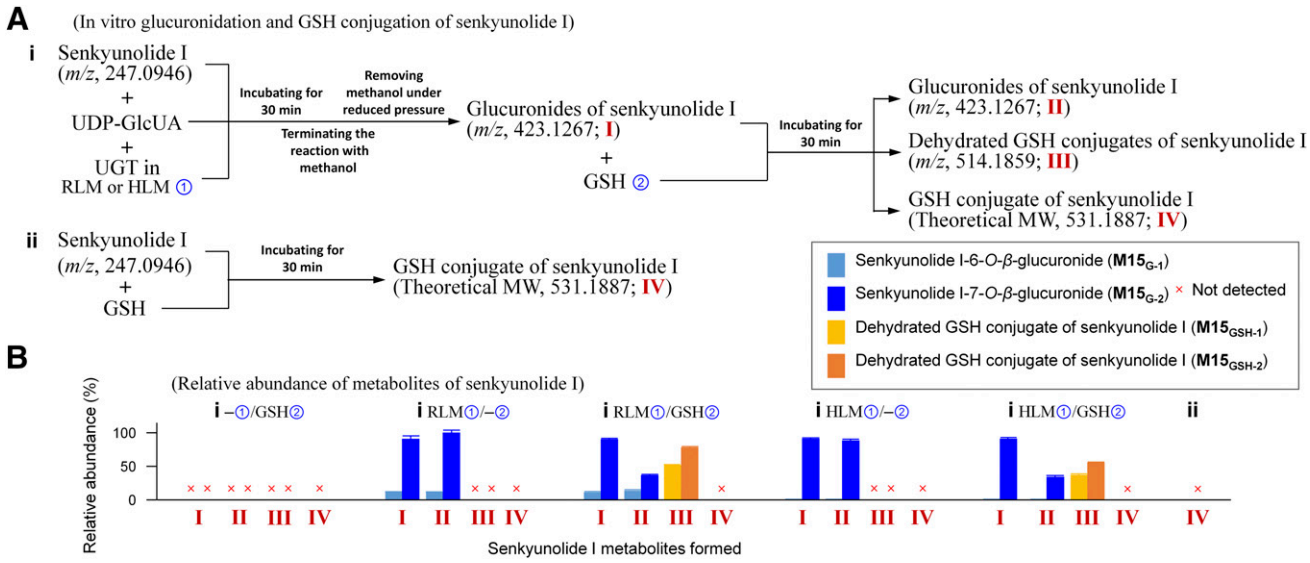

Fig. 4. Dehydrated GSH conjugates of senkyunolide I (**M15$_{GSH-1}$** and **M15$_{GSH-2}$**) formed in vitro by GSH replacement of glucuronic acid in a second metabolic reaction. (A) Experiments of in vitro glucuronidation and GSH conjugation of senkyunolide I. (B) Detection of metabolites of senkyunolide I and their relative abundance.

3-hydroxy-3-*n*-butylphthalide were also formed in vitro with UDP-GlcUA-fortified HLM and UDP-GlcUA-fortified RLM, but were negligibly detected in vivo. Figure 5 shows the proposed metabolic pathways of senkyunolides I (**15**) and G (**12**).

Pharmacokinetic Characteristics of Circulating XueBiJing Phthalides in Human Subjects and Rats. Figure 6 depicts the plasma concentration–time profiles of senkyunolides I (**15**) and G (**12**) in human subjects who intravenously received XueBiJing, and Table 3 summarizes their pharmacokinetic data. The circulating phthalides **15** and **12** exhibited dose- and injection-rate–dependent maximum plasma concentrations (C_{max}) and dose-dependent area under the concentration–time curve from 0 to infinity ($AUC_{0-\infty}$). Neither the C_{max} nor $AUC_{0-\infty}$ of phthalides **15** and **12** exhibited significant gender differences (P = 0.17–0.99) after correcting the compound doses for the subjects' body weights. The apparent volume of distribution at steady state (V_{SS}) and total plasma clearance ($CL_{tot,p}$) also showed no significant gender differences (P = 0.13–0.98). The mean V_{SS} of phthalide **15** for all the groups of dosage regimen was 13.2 times as much as that of phthalide **12** ($P = 2.7 \times 10^{-11}$), and the mean $CL_{tot,p}$ of phthalide **15** was 26.5 times as much as that of phthalide **12** ($P = 5.2 \times 10^{-11}$). The mean terminal $t_{1/2}$ of phthalide **12** was 2.7 times as much as that of phthalide **15** ($P = 3.7 \times 10^{-23}$). Apart from the glomerular filtration, tubular reabsorption was probably also involved in the renal excretion of phthalide **15**, as indicated by its mean ratio of renal clearance to the product of glomerular filtration rate and unbound fraction in plasma [CL_R/(GFR × f_u)] (Table 3). Such tubular

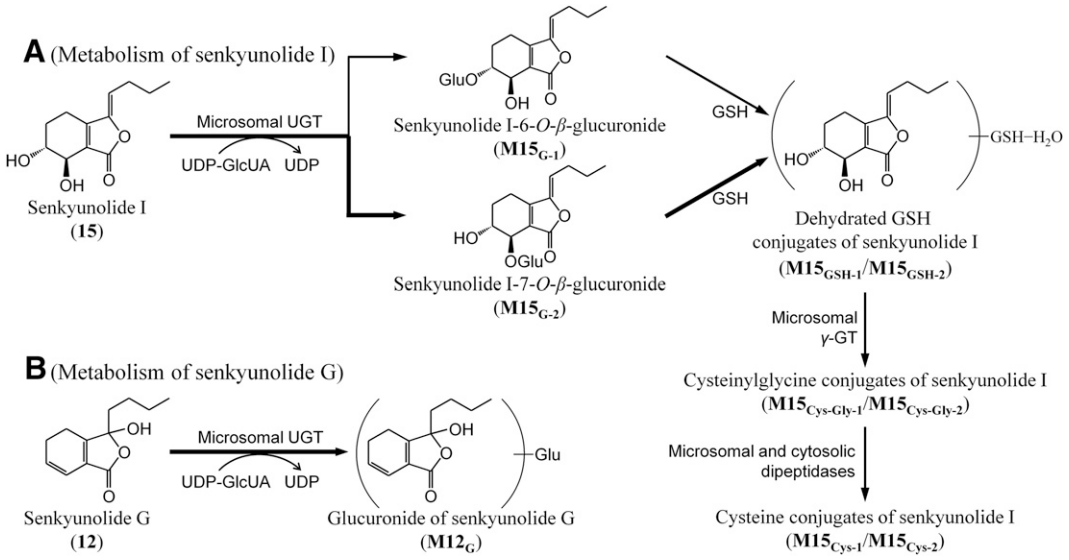

Fig. 5. Proposed metabolic pathways of (A) senkyunolide I (**15**) and (B) senkyunolide G (**12**) from intravenously dosed XueBiJing. Metabolite ID provides information regarding the parent compound, metabolite type, and metabolite isomer. For instance, M15 in **M15$_{G-1}$** denotes that the compound is a metabolite of senkyunolide I (**15**). The subscript letter G denotes glucuronide, and the subscript number 1 denotes the first eluted metabolite isomer. The subscript letters GSH, Cys-Gly, and Cys denote dehydrated glutathione conjugate, cysteinylglycine conjugate, and cysteine conjugate, respectively. **M12$_G$** indicates that only one senkyunolide G glucuronide was detected. Glu, glucuronosyl; γ-GT, γ-glutamyl transpeptidase; UDP, uridine 5′-diphosphate; UGT, uridine 5′-diphosphoglucuronosyltransferase.

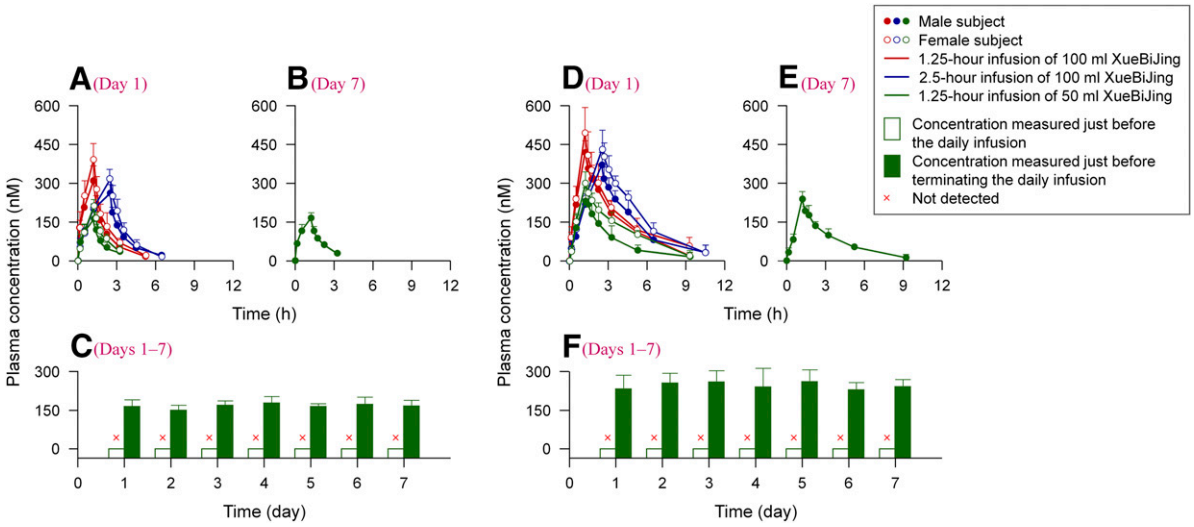

Fig. 6. Mean plasma concentrations of (A–C) senkyunolide I (**15**) and (D–F) senkyunolide G (**12**) over time in human subjects. (A and D) Day 1 data from human subjects who received a 1.25-hour intravenous infusion of 100 ml of XueBiJing (n = 12), a 2.5-hour infusion of 100 ml of XueBiJing (n = 12), or a 1.25-hour infusion of 50 ml of XueBiJing (n = 12). (B and E) Day 7 data from the six male subjects who received a 1.25-hour intravenous infusion of a 50-ml preparation of XueBiJing each day for 7 consecutive days. (C and F) Daily maximum plasma concentration in human subjects who received a 1.25-hour intravenous infusion of a 50-ml preparation of XueBiJing each day for 7 consecutive days (n = 6).

reabsorption might be a reason for the nondetection of phthalide **12** in urine. During subchronic daily intravenous infusions of XueBiJing for 7 consecutive days, accumulation of circulating phthalides **15** and **12** appeared to be negligible (Fig. 6; Supplemental Table 6).

Rat studies were designed to obtain some additional pharmacokinetic information that, for ethics reasons, was not obtainable via the human study but that is important to better understand the pharmacokinetics and disposition of XueBiJing compounds. Similarities and differences between humans and rats in pharmacokinetics of XueBiJing phthalides were considered (Supplemental Table 7), and further rat studies focused on senkyunolide I (**15**) due to the interspecies similarity. The rat systemic exposure to phthalide **15** (C_{max} and $AUC_{0-\infty}$) increased proportionally as the dose of XueBiJing increased from 10 to 90 ml/kg, while the V_{SS}, $CL_{tot,p}$, and $t_{1/2}$ remained basically constant (Fig. 7; Table 4). The effects of the matrix components of the preparation on the pharmacokinetics of phthalide **15** were assessed in rats by comparing the pharmacokinetic parameters obtained for the compound after dosing XueBiJing with those after dosing an injectable solution of purified

TABLE 3

Pharmacokinetics of senkyunolides I (**15**) and G (**12**) in human subjects who received an intravenous infusion of XueBiJing

The details of human pharmacokinetic study are described in the Supplemental Materials and Methods (Human Pharmacokinetic Study of XueBiJing). Senkyunolide G (**12**) was not detected in human urine after dosing XueBiJing. The data represent the mean ± S.D. For both phthalides, no significant gender differences in maximum plasma concentration (C_{max}), area under concentration–time curve from 0 to infinity ($AUC_{0-\infty}$), apparent volume of distribution at steady state (V_{SS}), or total plasma clearance ($CL_{tot,p}$) were observed after dose correction for the subjects' body weights (P = 0.13–0.99).

Pharmacokinetic Parameter	Dosage Regimen 1 (1.25-hour infusion, 100 ml/day)		Dosage Regimen 2 (2.5-hour infusion, 100 ml/day)		Dosage Regimen 3 (1.25-hour infusion, 50 ml/day)	
	Male (n = 6)	Female (n = 6)	Male (n = 6)	Female (n = 6)	Male (n = 6)	Female (n = 6)
Senkyunolide I (**15**)						
C_{max} (nM)	313 ± 57 (At 1.25 h after starting the infusion, but before terminating the infusion)	391 ± 63	262 ± 31 (At 2.5 h after starting the infusion, but before terminating the infusion)	328 ± 31	165 ± 23 (At 1.25 h after starting the infusion, but before terminating the infusion)	212 ± 32
$AUC_{0-\infty}$ (nM·h)	571 ± 115	690 ± 144	713 ± 84	863 ± 97	280 ± 23	374 ± 66
$t_{1/2}$ (h)	0.87 ± 0.09	0.79 ± 0.12	0.87 ± 0.25	0.98 ± 0.13	0.68 ± 0.14	0.79 ± 0.11
MRT (h)	1.73 ± 0.14	1.69 ± 0.21	2.41 ± 0.25	2.65 ± 0.19	1.52 ± 0.19	1.79 ± 0.23
V_{SS} (l/kg)	1.28 ± 0.10	1.24 ± 0.14	1.45 ± 0.15	1.59 ± 0.09	1.13 ± 0.13	1.22 ± 0.23
$CL_{tot,p}$ (l/h per kilogram)	0.748 ± 0.096	0.746 ± 0.130	0.610 ± 0.116	0.605 ± 0.071	0.745 ± 0.064	0.683 ± 0.087
CL_R (l/h per kilogram)	0.030 ± 0.002	0.039 ± 0.014	0.025 ± 0.011	0.029 ± 0.007	0.021 ± 0.008	0.025 ± 0.004
$f_{e\text{-}U}$ (%)	4.13 ± 0.61	5.14 ± 1.28	4.27 ± 1.91	4.76 ± 0.73	3.71 ± 1.23	4.70 ± 1.16
$CL_R/(GFR \times f_u)$ ratio	0.51 ± 0.03	0.65 ± 0.23	0.42 ± 0.17	0.49 ± 0.11	0.35 ± 0.12	0.43 ± 0.06
Senkyunolide G (**12**)						
C_{max} (nM)	424 ± 44 (At 1.25 h after starting the infusion, but before terminating the infusion)	498 ± 98	379 ± 41 (At 2.5 h after starting the infusion, but before terminating the infusion)	437 ± 78	238 ± 52 (At 1.25 h after starting the infusion, but before terminating the infusion)	302 ± 45
$AUC_{0-\infty}$ (nM·h)	1503 ± 176	1799 ± 333	1622 ± 229	1978 ± 258	779 ± 284	1105 ± 209
$t_{1/2}$ (h)	2.18 ± 0.27	2.45 ± 0.42	2.31 ± 0.35	2.26 ± 0.45	1.91 ± 0.41	2.20 ± 0.51
MRT (h)	3.72 ± 0.32	4.08 ± 0.56	4.52 ± 0.52	4.54 ± 0.58	3.33 ± 0.52	3.79 ± 0.74
V_{SS} (l/kg)	0.10 ± 0.01	0.11 ± 0.01	0.12 ± 0.01	0.12 ± 0.01	0.09 ± 0.01	0.08 ± 0.01
$CL_{tot,p}$ (l/h per kilogram)	0.027 ± 0.002	0.028 ± 0.004	0.026 ± 0.005	0.026 ± 0.004	0.028 ± 0.007	0.023 ± 0.004

CL_R, renal clearance; $f_{e\text{-}U}$, fractional urinary excretion; f_u, unbound fraction of compound in plasma; GFR, glomerular filtration rate; MRT, mean residence time.

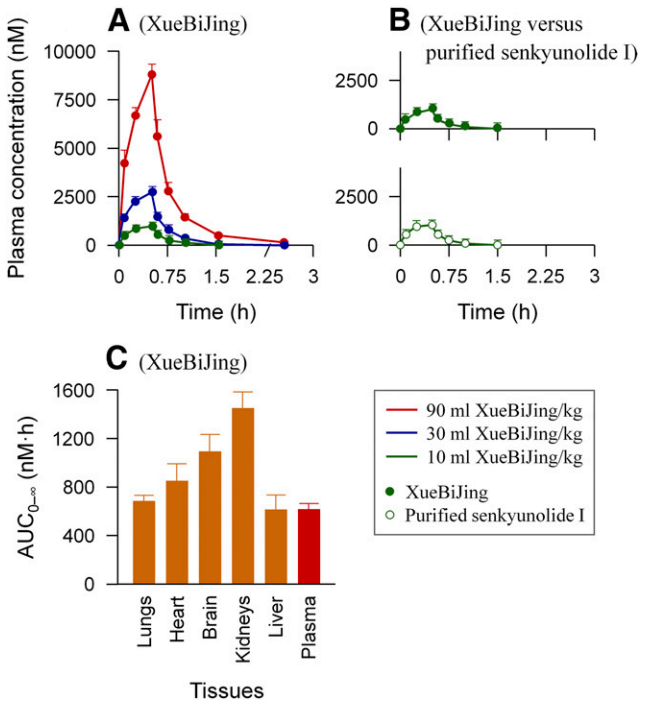

Fig. 7. Mean plasma concentrations and tissue exposure levels over time of senkyunolide I (**15**) in rats that received XueBiJing or an injectable solution of purified senkyunolide I. (A) Rats received a 0.5-hour intravenous infusion of XueBiJing at 10, 30, or 90 ml/kg (n = 6). (B) Rats received a 0.5-hour intravenous infusion of XueBiJing at 10 ml/kg (each milliliter of XueBiJing containing 0.3 μmol of phthalide **15**) or an injectable solution of purified senkyunolide I at 3.0 μmol/kg (n = 6). (C) Tissue and systemic exposure to unchanged phthalide **15** in rats that received an intravenous bolus dose of XueBiJing at 10 ml/kg (n = 5, for each time point). The AUC-based partition coefficients (K_P) of unchanged phthalide **15** between tissues and plasma were 1.10, 1.39, 1.80, 2.39, and 0.99 for the lungs, heart, brain, kidneys, and liver, respectively.

senkyunolide I. Other compounds in XueBiJing exhibited limited influence on the pharmacokinetics of phthalide **15** (Fig. 7; Supplemental Table 8). Consistent with its large V_{SS} in rats, phthalide **15** distributed extensively into rat lungs, heart, brain, kidneys, and liver (Fig. 7).

Table 5 summarizes pharmacokinetic data related to the in vivo reach of circulating XueBiJing phthalides. Senkyunolides I (**15**), G (**12**), H (16), and N (17), and 3-hydroxy-3-*n*-butylphthalide (10) exhibited good membrane permeability, as indicated by their Caco-2-based apparent permeability coefficients (P_{app}). However, the extent of their binding in human plasma was quite different, as indicated by their f_u. Notably, senkyunolide G was selectively bound to albumin rather than to other human plasma proteins (i.e., α_1-acid glycoprotein, γ-globulins, high-density lipoproteins, low-density lipoproteins, and very-low-density lipoproteins), as indicated by the proteins' relative binding capabilities (Table 6).

Discussion

In China, herbal medicines are extensively used in clinics and prescribed by both Western medicine physicians and traditional Chinese medicine (TCM) physicians. An ambitious attempt is under way to develop Chinese herbal medicines in line with modern standards, and the annual gross domestic product of the Chinese TCM pharmaceutical industry has increased from 23 billion RMB (about US$ 3.5 billion) in 1996 to 786 billion RMB (US$ 121 billion) in 2015 (Zhang and Chen, 2016). Currently, China FDA requires herbal medicines to be proved safe and effective before marketing. However, before the current period, Chinese herbal medicines having therapeutic claims largely based on their established use in TCM generally were approved without extensive testing, owing to the science and technology available at the time. Recently, a number of patent herbal medicines, manufactured by major Chinese TCM pharmaceutical companies, have shown therapeutic benefits in rigorous clinical studies similar to those for contemporary pharmaceuticals (Wang et al., 2011; Li et al., 2013; Shang et al., 2013; Zhang et al., 2014). Because of the complex chemical composition of such medicines, an adequate assessment of their efficacy and safety needs not only clinical studies but also identification of the medicines' chemical basis responsible for their therapeutic actions. Hence, pharmacokinetic research on Chinese herbal medicines, particularly those with proved efficacy and safety, has been proposed to serve as a crucial step in identifying such chemical basis (Lu et al., 2008; Liu et al., 2009; Hu et al., 2013; Cheng et al., 2016a). This pharmacokinetics-guided strategy is new and could be more successful than the classic phytochemistry-initiated strategy.

As a part of our ongoing serial pharmacokinetic research on XueBiJing, this investigation focused on the phthalides originating from the component herbs Chuanxiong and Danggui. We proceeded in two steps: 1) identifying the major circulating phthalides after dosing XueBiJing and 2) investigating the pharmacokinetic factors important for their pharmacodynamic effects, mainly in their in vivo reach, and the factors governing their systemic exposure. As a result, unchanged senkyunolides I (**15**) and G (**12**) were identified in human subjects as the major circulating phthalides out of the 10 phthalides detected in the

TABLE 4

Plasma pharmacokinetics of senkyunolide I (**15**) in rats that received a 0.5-hour intravenous infusion of XueBiJing at 10, 30, or 90 ml/kg and summary of the results from the dose proportionality assessment

The details of the rat pharmacokinetic study are described in the Supplemental Materials and Methods (Supportive Rat Pharmacokinetic Studies of XueBiJing). The data represent the mean ± S.D. Correlation was statistically significant with $P < 0.05$. The critical interval was 0.90–1.10 for the plasma pharmacokinetic data of phthalide **15**. The term "linear" was concluded statistically if the 90% confidence interval (90% CI) for slope was contained completely within the critical interval; "inconclusive" was concluded statistically if the 90% CI lay partly within the critical interval; "nonlinear" was concluded statistically if the 90% CI was entirely outside the critical interval.

Pharmacokinetic Parameter	Assessment of Plasma Pharmacokinetics			Assessment of Dose Proportionality			
	10 ml/kg (n = 6)	30 ml/kg (n = 6)	90 ml/kg (n = 6)	r	P	Slope (90% CI)	Conclusion
C_{max} (nM)	990 ± 106	2722 ± 262	8838 ± 536	0.99	1.8×10^{-17}	1.00 (0.95–1.04)	Linear
$AUC_{0-\infty}$ (nM·h)	574 ± 71	1628 ± 135	5560 ± 499	0.99	5.2×10^{-17}	0.99 (0.99–1.08)	Linear
$t_{1/2}$ (h)	0.19 ± 0.03	0.21 ± 0.01	0.24 ± 0.02	—	—	—	—
MRT (h)	0.45 ± 0.03	0.48 ± 0.02	0.53 ± 0.02	—	—	—	—
V_{SS} (l/kg)	2.19 ± 0.11	2.39 ± 0.15	2.28 ± 0.15	—	—	—	—
$CL_{tot,p}$ (l/h per kilogram)	4.853 ± 0.545	5.019 ± 0.411	4.396 ± 0.417	—	—	—	—

$AUC_{0-\infty}$, area under concentration–time curve from 0 to infinity; $CL_{tot,p}$, total plasma clearance; C_{max}, maximum plasma concentration; MRT, mean residence time; V_{SS}, apparent volume of distribution at steady state.

TABLE 5

Pharmacokinetic data related to in vivo reach of circulating XueBiJing phthalides

The details of in vitro pharmacokinetic studies are described in the Supplemental Materials and Methods (Supportive In Vitro Characterizations of Phthalides). The quoted volumes of total body water, intracellular fluids, extracellular fluids, and plasma for a 70-kg man are 0.60, 0.34, 0.26, and 0.04 l/kg, respectively; whereas such volumes for a 0.25-kg rat are 0.67, 0.37, 0.30, and 0.03 l/kg, respectively (Davies and Morris, 1993). XueBiJing compounds with volume of distribution at steady state (V_{SS}) in a human larger than 0.26 l/kg are predicted to have intracellular reach. Membrane permeability was determined based on apparent permeability coefficient (P_{app}) value of the compound measured on Caco-2 cell monolayers, with a P_{app} value $< 0.2 \times 10^{-6}$, 0.2×10^{-6}–2.8×10^{-6}, and $> 2.8 \times 10^{-6}$ cm/s indicating low, intermediate, and high membrane permeability, respectively (Li et al., 2012).

Compound	V_{SS}		Detection in Rat Brain	f_u		Membrane Permeability, Caco-2 Cell-based P_{app} (EfR)	B/P Ratio	
	Human	Rat		Human (%)	Rat (%)		Human	Rat
	l/kg							
Senkyunolide I (**15**)	1.18 ± 0.17	2.19 ± 0.11	Detected; K_P, 1.8	53.6	48.3	Good, 39.0×10^{-6} (1.2)	0.69	0.82
Senkyunolide G (**12**)	0.09 ± 0.01	0.85 ± 0.10	Not detected	3.0	13.3	Good, 27.8×10^{-6} (1.4)	0.62	0.61
Senkyunolide H (**16**)	1.19 ± 0.12	2.02 ± 0.06	Detected; K_P, 1.0	49.8	48.1	Good, 34.7×10^{-6} (1.3)	NM	0.78
Senkyunolide N (**17**)	0.98 ± 0.26	1.18 ± 0.07	Detected; K_P, 1.4	76.0	74.6	Good, 17.3×10^{-6} (1.4)	NM	0.90
3-Hydroxy-3-*n*-butylphthalide (**10**)	0.22 ± 0.04	0.64 ± 0.12	Not detected	17.9	18.1	Good, 3.62×10^{-6} (2.4)	NM	0.74

B/P ratio, blood-to-plasma concentration ratio; EfR, efflux ratio; f_u, unbound fraction of compound in plasma; K_P, AUC-based partition coefficient of compound between brain and plasma; NM, not measured.

dosed XueBiJing. However, phthalides **15** and **12** exhibited different pharmacokinetic characteristics. Although both the phthalides had good membrane permeability, their binding in human plasma was quite different. This difference, together with the significant differences in V_{SS}, suggest that these two phthalides could differ in their in vivo reach. After dosing XueBiJing, phthalide **15** was extensively distributed and could well reach both extracellular and intracellular receptors. Among the major circulating herbal compounds identified in our pharmacokinetic research on XueBiJing, phthalide **15** was the only XueBiJing compound well detected in rat brain, suggesting its good brain penetration. This finding may be important because XueBiJing is used in the treatment of patients with sepsis showing brain dysfunction. In contrast, phthalide **12** resided largely in plasma; this probably limited its bioavailability to act on therapeutic targets. Phthalides **15** and **12** also substantially differed in $CL_{tot,p}$. Clearance of phthalide **15** from the systemic circulation was rapid and was governed mainly by glucuronidation. Clearance of phthalide **12** from the systemic circulation was quite slow, probably due to very slow glucuronidation in humans. The significantly smaller V_{SS} and lower $CL_{tot,p}$ of phthalide **12**, relative to phthalide **15**, resulted in its higher levels of systemic exposure in humans, even though its dose from XueBiJing was only 15% of that of phthalide **15**. It is worth mentioning that the high exposure level of phthalide **12** represented its total (bound and unbound) concentration, predominantly comprising the bound concentration rather than the bioavailable unbound concentration.

Sepsis is a complex, heterogeneous, and rapidly evolving life-threatening syndrome; diagnostic and prognostic biomarkers have been used to assist clinicians in treatment decisions (Sandquist and Wong, 2014; Jensen and Bouadma, 2016). However, due to their considerable delay and their insufficient specificity and sensitivity for routine employment in clinical practice, classic biomarkers for sepsis care need to be supplemented with new markers. Pharmacokinetic research on an herbal medicine can help identify pharmacokinetic markers originating from the medicine. One type of such markers can reflect the body exposure to the herbal compounds responsible for or related to the medicine's therapeutic action and the associated influencing factors (Lu et al., 2008; Hu et al., 2013; Li, 2017) (Supplemental Table 9). Proposed here is another type of pharmacokinetic markers that can reflect and predict abnormal cellular processes in tissues and treatment-caused reversion toward normal states; these herbal compounds should exhibit pharmacokinetics and disposition that could be detectably altered in response to the disease. In this investigation, hepatic glucuronidation of

TABLE 6

Binding of senkyunolides I and G to individual proteins of human plasma and the proteins' relative binding capabilities

The details of the in vitro pharmacokinetic study are described in the Supplemental Materials and Methods [Assessment of Protein Binding (Total Plasma and Individual Proteins)]. The binding percentage in isolated plasma protein solution represents the mean ± S.D.

Human Plasma Protein	[P]	Binding Percentage in Isolated Plasma Protein Solution (%)	nK	nK × [P]: Binding Capability	Relative Binding Capability (%)[a]
	μM		*1/μM*		
Senkyunolide I					
Albumin	600	40.5 ± 3.5	0.001	0.68	48.6
α_1-Acid glycoprotein	10	5.8 ± 3.2	0.009	0.09	6.4
γ-Globulins	80	8.7 ± 3.2	0.001	0.12	8.3
High-density lipoproteins	10	6.6 ± 3.9	0.013	0.13	9.2
Low-density lipoproteins	1	18.8 ± 4.3	0.260	0.26	18.2
Very-low-density lipoproteins	0.1	6.7 ± 3.6	1.300	0.13	9.3
Senkyunolide G					
Albumin	600	98.7 ± 0.4	0.095	56.7	99.0
α_1-Acid glycoprotein	10	4.7 ± 2.8	0.009	0.09	0.2
γ-Globulins	80	5.4 ± 2.3	0.001	0.05	0.1
High-density lipoproteins	10	3.7 ± 2.6	0.006	0.06	0.1
Low-density lipoproteins	1	8.2 ± 1.7	0.120	0.12	0.2
Very-low-density lipoproteins	0.1	12.1 ± 5.3	2.600	0.26	0.4

nK, total binding constant; [P], reported protein concentration in human plasma under physiologic conditions (Urien et al., 1992).

[a]Calculated by $\{(nK_{protein} \times [protein])/(nK_{albumin} \times [albumin] + nK_{\alpha 1\text{-acid glycoprotein}} \times [\alpha_1\text{-acid glycoprotein}] + nK_{\gamma\text{-globulins}} \times [\gamma\text{-globulins}] + nK_{high\text{-density lipoproteins}} \times [high\text{-density lipoproteins}] + nK_{low\text{-density lipoproteins}} \times [low\text{-density lipoproteins}] + nK_{very\text{-low-density lipoproteins}} \times [very\text{-low-density lipoproteins}])\} \times 100\%$.

senkyunolide I (**15**) was found to be mediated primarily by UGT2B15; the resulting glucuronides (**M15$_{G-1}$** and **M15$_{G-2}$**) were electrophilic and conjugated with GSH. Senkyunolide G (**12**) was found to be selectively and extensively bound to albumin in human plasma. Sepsis is accompanied by profound changes in patients, including hepatic, renal, and circulatory dysfunction, impaired hepatic synthesis of GSH, and altered albumin concentration and structure (Gatta et al., 2012; Bosmann and Ward, 2013; Blot et al., 2014). In addition, growing evidence has shown that inflammation and immune responses may result in down-regulation of drug-metabolizing enzymes and transporters (Congiu et al., 2002; Aitken et al., 2006; Harvey and Morgan, 2014). Accordingly, potential exists for septic-pathophysiology-induced alterations in the pharmacokinetics and disposition of phthalides **15** and **12** and for reversion to a normal xenobiotic disposition state when the sepsis burden is substantially reduced in patients across the time course of treatment. Our pilot analysis of XueBiJing compounds in plasma samples from patients with sepsis indicated that unchanged phthalide **15** (exhibiting increased systemic exposure in patients, relative to healthy human subjects), **M15$_{G-2}$** (being detectable in patients, but not in healthy human subjects), and phthalide **12** (exhibiting an increased f_u in patients, relative to healthy human subjects) could serve as pharmacokinetic markers reflecting the patients' down-regulated UGT2B15, impaired hepatic synthesis of GSH, and decreased plasma albumin, respectively (data not shown).

Similar to synthetic drug discovery and development, the driving motivation for and primary goal of scientific research on Chinese herbal medicines, including pharmacokinetic investigation, is to enrich therapeutic armamentarium, especially for multifactorial diseases. XueBiJing, as an add-on therapy, is promising for modulating the septic response, as shown by many clinical and experimental studies. In summary, among multiple phthalides in XueBiJing, unchanged senkyunolides I (**15**) and G (**12**) are the major circulating phthalides, but their different pharmacokinetics in humans might influence their contribution to the medicine's therapeutic action. Based on this pharmacokinetic investigation and such investigations of XueBiJing's other component herbs, follow-up pharmacodynamic assessments of various XueBiJing compounds, (unchanged and metabolized), are planned, with respect to antisepsis-related antiinflammatory, immunomodulatory, anticoagulant, and endothelium-protective activities. UGT2B15-mediated hepatic glucuronidation of phthalide **15** is the elimination route governing its clearance from the systemic circulation and the resulting electrophilic glucuronides are conjugated with GSH in the liver. Phthalide **12** is selectively and extensively bound to albumin in human plasma. These disposition characteristics of the phthalides could be altered by septic pathophysiology. An additional study in patients with sepsis is planned for XueBiJing to investigate influences of sepsis on pharmacokinetics of bioactive herbal compounds and to identify pharmacokinetic markers to supplement classic biomarkers for sepsis care. Interestingly, senkyunolide I has been identified, to our knowledge, as the most selective substrate ever reported for human UGT2B15 (Court et al., 2002; Rowland et al., 2013), and senkyunolide G was found to be selectively bound to human plasma albumin. These naturally occurring phthalides could be useful tool compounds in drug metabolism and pharmacokinetic studies and clinical studies.

Authorship Contributions

Participated in research design: C. Li, Nating Zhang.

Conducted experiments: Nating Zhang, Cheng, Olaleye, Sun, L. Li, Huang, Du, Yang, Wang, Shi, Xu, Y. Li, Wen, Naixia Zhang.

Performed data analysis: C. Li, Nating Zhang.

Wrote or contributed to the writing of the manuscript: C. Li, Nating Zhang, Olaleye.

References

Aitken AE, Richardson TA, and Morgan ET (2006) Regulation of drug-metabolizing enzymes and transporters in inflammation. *Annu Rev Pharmacol Toxicol* **46**:123–149.

Blot SI, Pea F, and Lipman J (2014) The effect of pathophysiology on pharmacokinetics in the critically ill patient—concepts appraised by the example of antimicrobial agents. *Adv Drug Deliv Rev* **77**:3–11.

Bosmann M and Ward PA (2013) The inflammatory response in sepsis. *Trends Immunol* **34**: 129–136.

Chen F, Li L, Xu F, Sun Y, Du F-F, Ma X-T, Zhong C-C, Li X-X, Wang F-Q, Zhang N-T, et al. (2013) Systemic and cerebral exposure to and pharmacokinetics of flavonols and terpene lactones after dosing standardized *Ginkgo biloba* leaf extracts to rats via different routes of administration. *Br J Pharmacol* **170**:440–457.

Chen Y and Li C-S (2013) The effectiveness of XueBiJing injection in therapy of sepsis: a multicenter clinical study. *Zhonghua Jizhen Yixue Zazhi* **22**:130–135.

Cheng C, Du F, Yu K, Xu F, Wang F, Li L, Olaleye OE, Yang J, Chen F, Zhong C, et al. (2016a) Pharmacokinetics and disposition of circulating iridoids and organic acids in rats intravenously receiving ReDuNing injection. *Drug Metab Dispos* **44**:1853–1858.

Cheng C, Lin J-Z, Li L, Yang J-L, Jia W-W, Huang Y-H, Du F-F, Wang F-Q, Li M-J, Li Y-F, et al. (2016b) Pharmacokinetics and disposition of monoterpene glycosides derived from *Paeonia lactiflora* roots (Chishao) after intravenous dosing of antiseptic XueBiJing injection in human subjects and rats. *Acta Pharmacol Sin* **37**:530–544.

Chinese Society of Critical Care Medicine (2015) Chinese guidelines for management of severe sepsis and septic shock 2014. *Zhonghua Wei Zhong Bing Ji Jiu Yi Xue* **27**:401–426.

Cohen J, Vincent J-L, Adhikari NKJ, Machado FR, Angus DC, Calandra T, Jaton K, Giulieri S, Delaloye J, Opal S, et al. (2015) Sepsis: a roadmap for future research. *Lancet Infect Dis* **15**: 581–614.

Congiu M, Mashford ML, Slavin JL, and Desmond PV (2002) UDP glucuronosyltransferase mRNA levels in human liver disease. *Drug Metab Dispos* **30**:129–134.

Court MH, Duan S-X, Guillemette C, Journault K, Krishnaswamy S, Von Moltke LL, and Greenblatt DJ (2002) Stereoselective conjugation of oxazepam by human UDP-glucuronosyltransferases (UGTs): *S*-oxazepam is glucuronidated by UGT2B15, while *R*-oxazepam is glucuronidated by UGT2B7 and UGT1A9. *Drug Metab Dispos* **30**:1257–1265.

Dai J-Y, Yang J-L, and Li C (2008) Transport and metabolism of flavonoids from Chinese herbal remedy Xiaochaihu- tang across human intestinal Caco-2 cell monolayers. *Acta Pharmacol Sin* **29**:1086–1093.

Davies B and Morris T (1993) Physiological parameters in laboratory animals and humans. *Pharm Res* **10**:1093–1095.

Dong T-H, Zhang G-P, Dong K, Liu S, and Yao Y-M (2016) Research progress of mechanism of action of XueBiJing injection in the treatment of sepsis. *Chin J Tradit Chin Med West Med Crit Care* **23**:554–557.

Feng Z, Lu Y, Wu X, Zhao P, Li J, Peng B, Qian Z, and Zhu L (2012) Ligustilide alleviates brain damage and improves cognitive function in rats of chronic cerebral hypoperfusion. *J Ethnopharmacol* **144**:313–321.

Gao J, Kong L, Liu S, Feng Z, Shen H, and Liu Q; Xuebijing Injection III Clinical Group (2015) A prospective multicenter clinical study of Xuebijing injection in the treatment of sepsis and multiple organ dysfunction syndrome. *Zhonghua Wei Zhong Bing Ji Jiu Yi Xue* **27**:465–470.

Gatta A, Verardo A, and Bolognesi M (2012) Hypoalbuminemia. *Intern Emerg Med* **7** (Suppl 3): S193–S199.

Guo B, Li C, Wang G, and Chen L (2006) Rapid and direct measurement of free concentrations of highly protein-bound fluoxetine and its metabolite norfluoxetine in plasma. *Rapid Commun Mass Spectrom* **20**:39–47.

Harvey RD and Morgan ET (2014) Cancer, inflammation, and therapy: effects on cytochrome p450-mediated drug metabolism and implications for novel immunotherapeutic agents. *Clin Pharmacol Ther* **96**:449–457.

Hu Z, Yang J, Cheng C, Huang Y, Du F, Wang F, Niu W, Xu F, Jiang R, Gao X, et al. (2013) Combinatorial metabolism notably affects human systemic exposure to ginsenosides from orally administered extract of *Panax notoginseng* roots (Sanqi). *Drug Metab Dispos* **41**:1457–1469.

Huang H, Ji L, Song S, Wang J, Wei N, Jiang M, Bai G, and Luo G (2011) Identification of the major constituents in Xuebijing injection by HPLC-ESI-MS. *Phytochem Anal* **22**:330–338.

Jensen J-U and Bouadma L (2016) Why biomarkers failed in sepsis. *Intensive Care Med* **42**: 2049–2051.

Li C (2017) Multi-compound pharmacokinetic research on Chinese herbal medicines: approach and methodology. *Zhongguo Zhongyao Zazhi* **42**:607–617.

Li L, Zhao Y-S, Du F-F, Yang J-L, Xu F, Niu W, Ren Y-H, and Li C (2012) Intestinal absorption and presystemic elimination of various chemical constituents present in GBE50 extract, a standardized extract of *Ginkgo biloba* leaves. *Curr Drug Metab* **13**:494–509.

Li X-X, Cheng C, Wang F-Q, Huang Y-H, Jia W-W, Olaleye OE, Li M-J, Li Y-F, and Li C (2016) Pharmacokinetics of catechols in human subjects intravenously receiving XueBiJing injection, an emerging antiseptic herbal medicine. *Drug Metab Pharmacokinet* **31**:95–98.

Li X, Zhang J, Huang J, Ma A, Yang J, Li W, Wu Z, Yao C, Zhang Y, Yao W, et al.; Efficacy and Safety of Qili Qiangxin Capsules for Chronic Heart Failure Study Group (2013) A multicenter, randomized, double-blind, parallel-group, placebo-controlled study of the effects of qili qiangxin capsules in patients with chronic heart failure. *J Am Coll Cardiol* **62**:1065–1072.

Liu H, Yang J, Du F, Gao X, Ma X, Huang Y, Xu F, Niu W, Wang F, Mao Y, et al. (2009) Absorption and disposition of ginsenosides after oral administration of *Panax notoginseng* extract to rats. *Drug Metab Dispos* **37**:2290–2298.

Liu Y-C, Yao F-H, Chai Y-F, Dong N, Sheng Z-Y, and Yao Y-M (2015) XueBiJing injection promotes M2 polarization of macrophages and improves survival rate in septic mice. *Evid Based Complement Alternat Med* **2015**:352642.

Lu T, Yang J, Gao X, Chen P, Du F, Sun Y, Wang F, Xu F, Shang H, Huang Y, et al. (2008) Plasma and urinary tanshinol from *Salvia miltiorrhiza* (Danshen) can be used as pharmacokinetic markers for cardiotonic pills, a cardiovascular herbal medicine. *Drug Metab Dispos* **36**: 1578–1586.

Or TCT, Yang CLH, Law AHY, Li JCB, and Lau ASY (2011) Isolation and identification of anti-inflammatory constituents from *Ligusticum chuanxiong* and their underlying mechanisms of action on microglia. *Neuropharmacology* **60**:823–831.
Qi H, Siu S-O, Chen Y, Han Y, Chu IK, Tong Y, Lau ASY, and Rong J (2010) Senkyunolides reduce hydrogen peroxide-induced oxidative damage in human liver HepG2 cells via induction of heme oxygenase-1. *Chem Biol Interact* **183**:380–389.
Reagan-Shaw S, Nihal M, and Ahmad N (2008) Dose translation from animal to human studies revisited. *FASEB J* **22**:659–661.
Rowland A, Miners JO, and Mackenzie PI (2013) The UDP-glucuronosyltransferases: their role in drug metabolism and detoxification. *Int J Biochem Cell Biol* **45**:1121–1132.
Sandquist M and Wong HR (2014) Biomarkers of sepsis and their potential value in diagnosis, prognosis and treatment. *Expert Rev Clin Immunol* **10**:1349–1356.
Shang H, Zhang J, Yao C, Liu B, Gao X, Ren M, Cao H, Dai G, Weng W, Zhu S, et al. (2013) Qi-shen-yi-qi dripping pills for the secondary prevention of myocardial infarction: a randomised clinical trial. *Evid Based Complement Alternat Med* **2013**:738391.
Singer M, Deutschman CS, Seymour CW, Shankar-Hari M, Annane D, Bauer M, Bellomo R, Bernard GR, Chiche J-D, Coopersmith CM, et al. (2016) The third international consensus definitions for sepsis and septic shock (sepsis-3). *JAMA* **315**:801–810.
Smith BP, Vandenhende FR, DeSante KA, Farid NA, Welch PA, Callaghan JT, and Forgue ST (2000) Confidence interval criteria for assessment of dose proportionality. *Pharm Res* **17**:1278–1283.
Song Y-L, Yao C, Shang H-C, Yao X-Q, and Bai C-X (2016) Late-breaking abstract: intravenous infusion of Chinese medicine XueBiJing significantly improved clinical outcome in severe pneumonia patients in a multiple center randomized controlled clinical trials. *Eur Respir J* **48**:OA3323.
Urien S, Claudepierre P, Meyer J, Brandt R, and Tillement J-P (1992) Comparative binding of etretinate and acitretin to plasma proteins and erythrocytes. *Biochem Pharmacol* **44**:1891–1893.
Wang C, Cao B, Liu Q-Q, Zou Z-Q, Liang Z-A, Gu L, Dong J-P, Liang L-R, Li XW, Hu K, et al. (2011) Oseltamivir compared with the Chinese traditional therapy maxingshigan-yinqiaosan in the treatment of H1N1 influenza: a randomized trial. *Ann Intern Med* **155**:217–225.
Williams AJ, Ekins S, Spjuth O, and Willighagen EL (2012) Accessing, using, and creating chemical property databases for computational toxicology modeling. *Methods Mol Biol* **929**: 221–241.
Yin Q and Li C (2014) Treatment effects of xuebijing injection in severe septic patients with disseminated intravascular coagulation. *Evid Based Complement Alternat Med* **2014**:949254.
Zhang B-L and Chen C-H (2016) *Mordernization of Chinese Medicine for Twenty Years: 1996–2015*, Shanghai Science & Technology Press, Shanghai.
Zhang L, Li P, Xing C-Y, Zhao J-Y, He Y-N, Wang J-Q, Wu X-F, Liu Z-S, Zhang A-P, Lin H-L, et al. (2014) Efficacy and safety of *Abelmoschus manihot* for primary glomerular disease: a prospective, multicenter randomized controlled clinical trial. *Am J Kidney Dis* **64**:57–65.

Address correspondence to: Dr. Chuan Li, Laboratory for DMPK Research of Herbal Medicines, Shanghai Institute of Materia Medica, Chinese Academy of Sciences, 501 Haike Road, Zhangjiang Hi-Tech Park, Shanghai 201203, China. E-mail: chli@simm.ac.cn

Pharmacokinetics-Based Identification of Potential Therapeutic Phthalides from XueBiJing, a Chinese Herbal Injection Used in Sepsis Management

Nating Zhang, Chen Cheng, Olajide E Olaleye, Yan Sun, Li Li, Yühong Huang, Feifei Du, Junling Yang, Fengqing Wang, Yanhong Shi, Fang Xu, Yanfen Li, Qi Wen, Naixia Zhang, and Chuan Li

Drug Metabolism and Disposition

Supplemental Materials and Methods

Drug Products, Chemicals, and Reagents. XueBiJing injection was manufactured by Tianjin Chasesun Pharmaceutical Co., Ltd. (Tianjin, China) with a China FDA drug ratification number of GuoYaoZhunZi-Z20040033. Each milliliter of XueBiJing is prepared from a combination of 0.1 g each of Honghua (*Carthamus tinctorius* flowers), Chishao (*Paeonia lactiflora* roots), Chuanxiong (*Ligusticum chuanxiong* rhizomes), Danggui (*Angelica sinensis* roots), and Danshen (*Salvia miltiorrhiza* roots), yielding an herb-to-injection ratio of 1:2. The final product of XueBiJing is a sterile and nonpyrogenic dosage form for intravenous administration and is standardized to contain 1.0–1.7 mg/ml paeoniflorin and 0.2–0.5 mg/ml hydroxysafflor yellow A.

Samples of nine lots (1309271, 1309281, 1309291, 1309301, 1405301, 1406161, 1408191, 1410081, and 1501181) of XueBiJing were obtained from Tianjin Chasesun Pharmaceuticals. XueBiJing from the lot 1309301 (manufacture, September 2013; expiration, March 2015) was used in human study and rat studies. To intravenously dose XueBiJing in rats at 30 and 90 ml/kg, the preparation (90 and 270 ml, respectively) was first lyophilized in-house to dryness and the resulting residue (0.59 and 1.77 g, respectively) was reconstituted in 30 ml of deionized water. In addition, an injectable solution of senkyunolide I was prepared, for dosing in rats, by dissolving the purified compound (3.64 mg) in the same vehicle (60 ml) as that for preparation of XueBiJing. Before dosing, the concentrated XueBiJing solution and the senkyunolide I solution, as well as XueBiJing, were analyzed with respect to the concentration of the phthalide.

Crude material samples of XueBiJing's component herbs Chuanxiong (*L. chuanxiong* rhizomes) and Danggui (*A. sinensis* roots), five lots for each, were obtained from Tianjin Chasesun Pharmaceuticals and were stored at −20°C until analysis.

Senkyunolides A, H, and I, 3-*n*-butylenephthalide, 3-*n*-butylphthalide, levistolide A, and *Z*-ligustilide were obtained from Shanghai Yuanye Bio-Technology Co., Ltd. (Shanghai, China) and senkyunolide G, senkyunolide N, and 3-hydroxy-3-*n*-butylphthalide were obtained from Shanghai Standard Technology Co., Ltd. (Shanghai, China); the compounds' purity was ≥ 98%. Chemical reagents and organic solvents were obtained from Sinopharm Chemical Reagent Co., Ltd. (Shanghai, China).

Normal saline (0.9% NaCl injection; China FDA drug ratification number, GuoYaoZhunZi-H12020025) used in this study was manufactured by China Otsuka Pharmaceutical Co., Ltd. (Tianjin, China). Isoflurane and sodium heparin were obtained from Sinopharm Chemical Reagent Co., Ltd. (Shanghai, China). Pentobarbital was obtained from Shanghai Westang Biotechnology (Shanghai, China). Pooled human liver microsomes (HLM) (20.0 mg protein/ml), prepared from Chinese male and female human livers, was obtained from Research Institute for Liver Diseases (Shanghai) Co., Ltd. (Shanghai, China), while pooled rat liver microsomes (RLM) (8.5 mg protein/ml) was prepared from livers of male Sprague-Dawley rats in-house by differential centrifugation. cDNA-expressed human uridine 5′-diphosphoglucuronosyltransferase (UGT) enzymes UGT1A1, UGT1A3, UGT1A4, UGT1A6, UGT1A7, UGT1A8, UGT1A9, UGT1A10, UGT2B4, UGT2B7, UGT2B10, UGT2B15, and UGT2B17 were obtained from Corning Gentest (Woburn, MA). Before use, HLM and RLM, and cDNA-expressed human UGT isoforms were evaluated, with respect to their glucuronidation activities, using the known substrates: 4-methylumbelliferone for HLM and RLM, UGT1A1, UGT1A3, UGT1A6, UGT1A7, UGT1A8, UGT1A9, UGT1A10, UGT2B7, UGT2B15, and UGT2B17, trifluoperazine for UGT1A4, and eugenol for UGT2B4 and UGT2B10. Reduced GSH, UDP-GlcUA, alamethicin, Tris-base, 4-methylumbelliferone, trifluoperazine, eugenol, antipyrine, atenolol, indomethacin, novobiocin, rhodamine 123, sulfasalazine, verapamil, taurocholic acid, imatinib, Hank's buffered salt solution, and human plasma γ-globulins were obtained from Sigma-Aldrich (St. Louis, MO). Anlotinib was obtained from TCI Chemicals (Shanghai, China). BSA was obtained from J&K Scientific (Beijing, China). Human colonic adenocarcinoma cells (Caco-2 cells) were obtained from American Type Culture Collection (Manassas, VA). Dulbecco's modified Eagle's medium, minimal essential medium nonessential amino acids, and penicillin-streptomycin were obtained from Gibco Invitrogen Cell Culture (Grand Island, NY). FBS was obtained from HyClone Laboratories (Logan, UT). Human plasma albumin, α_1-acid glycoprotein, high density lipoproteins, low density lipoproteins, and very low density lipoproteins were obtained from Athens Research & Technology (Athens, GA). Before use, the binding activities of the isolated human plasma proteins were evaluated with known ligands, i.e., anlotinib for albumin, high density lipoproteins, low density lipoproteins, and very low density lipoproteins and imatinib for α_1-acid glycoprotein and γ-globulins (Zhong et al., 2017). Deuterated dimethyl sulfoxide (D, 99.9%; containing 0.03% v/v tetramethylsilane) was obtained from Cambridge Isotope Laboratories, Inc. (Andover, MA).

Human Pharmacokinetic Study of XueBiJing. A single-center, open-label human study of XueBiJing was performed at the National Clinical Research Center of the Second Affiliated Hospital of Tianjin University of Traditional Chinese Medicine (Tianjin, China). The study procedure was approved by an ethics committee of clinical investigation at the hospital, and had been carried out in accordance with the Declaration of Helsinki. The study was registered at the Chinese Clinical Trials Registry (www.chictr.org.cn) with a registration number of ChiCTR-ONRC-13003932. Subjects were healthy men and women (18–35 years of age; 19–24 kg/m^2 of body mass index) with no active medical illness by history, physical, or laboratory evaluation. Subjects were excluded if they were allergic to any products prepared from the component herbs of XueBiJing. No other medications were allowed two weeks prior to and throughout the study period. All subjects gave written informed consent prior to participation in the study.

Human subjects were randomly divided into three groups, stratified by sex, and each group had six male and six female subjects. The subjects received a single dose of XueBiJing and the dosage regimens were one of the following: (1) a single 1.25-h infusion of 100-ml preparation (diluted with 100 ml of 0.9% NaCl injection), (2) a single 2.5-h infusion of 100-ml preparation (diluted with 200 ml of 0.9% NaCl injection), or (3) a single 1.25-h infusion of 50-ml preparation (diluted with 100 ml of 0.9% NaCl injection). The test dosage regimens were designed according to the label dose of XueBiJing (100 ml/time/person) at infusion rate that is commonly used for XueBiJing in clinics to treat patients with sepsis (regimen 1) and the label doses of XueBiJing (50 and 100 ml/time/person) at infusion rate that is generally recommended for intravenous administration of Chinese herbal injections (regimens 2 and 3). The infusion was implemented using ZNB-XB intelligent infusion pump (Beijing, China). For regimens 1 and 3, serial blood samples (around 3 ml each time) were collected, from an antecubital vein catheter, before and 0.17, 0.5, 1.25 (just before terminating the infusion), 1.42, 1.75, 2.25, 3.25, 5.25, 9.25, and 24 h after starting the infusion. For regimen 2, the time schedule of blood sampling was before and 0.17, 0.5, 1.25, 2.5 (just before terminating the infusion), 2.67, 3, 3.5, 4.5, 6.5, 10.5, and 24 h after starting the infusion. Serial urine samples were collected from the subjects; the sampling time schedules were the same for all the regimens, i.e., before and 0–3, 3–6, 6–10, and 10–24 h after starting the infusion. In addition, the six male subjects of regimen 3 continued to receive the same dose of XueBiJing each day for the following six days; the time schedules for blood samplings on day 2–6 were before and 1.25 h (just before terminating the infusion) after the daily infusion was started and those for blood and urine samplings on day 7 were the same as those on day 1. All blood samples were heparinized and centrifuged to obtain the plasma fractions, and all urine samples were immediately weighed after collection. Human plasma and urine samples were stored at −70°C, without use of any preservative, until analysis. The time schedules for dosing and sampling in this human pharmacokinetic study are also summarized in Supplemental Table 1.

Supportive Rat Pharmacokinetic Studies of XueBiJing. All animal care and experimental procedures complied with the Guide for the Care and Use of Laboratory Animals adopted and promulgated by the U.S. National Institutes of Health and were reviewed and approved by the Institutional Animal Care and Use Committee at Shanghai Institute of Materia Medica (Shanghai, China). Male Sprague-Dawley rats (230–270 g, 6–8 weeks; Sino-British SIPPR/BK Laboratory Animal Co., Ltd., Shanghai, China) were housed in standard cages under specific pathogen free conditions in a unidirectional airflow room at 20–24 ℃, relative humidity of 30–70% with a 12-h light/dark cycle and were given filtered tap water and commercial rat chow *ad libitum*. Rats were allowed to acclimate to the facilities and environment for three days before use. Rats received in-house femoral-vein-cannulation for infusion of XueBiJing and other test solutions. In addition, some of the rats also received in-house either femoral-artery-cannulation for blood sampling or bile-duct-cannulation for bile sampling (Chen et al., 2013). After the surgery, rats were housed individually and allowed to regain their preoperative body weights. During the bile collection period, a sodium taurocholate solution (pH 7.4; 36 ml) was infused into the duodena of rats at 1.5 ml/h. All the rats, except those used in tissue distribution study, were euthanized with CO_2 after use. A total of 62 rats were used in the experiments described here.

The first study was a single ascending dose study and 18 rats were randomly assigned to three groups (six rats per group). Each group received a single 0.5-h intravenous infusion of XueBiJing at 10, 30, or 90 ml/kg. The dose 10 ml/kg (at around 2.5 ml per rat) for rats was derived from the label dose of XueBiJing for patients (100 ml/time/person) according to dose normalization by body surface area (Reagan-Shaw et al., 2008). The doses 30 and 90 ml/kg were given, also at around 2.5 ml/rat, by reconstituting the lyophilized preparation in deionized water. Serial blood samples (around 80 μl each time) were collected before and 0.08, 0.25, 0.5 (just before terminating the infusion), 0.58, 0.75, 1, 1.5, 2.5, 4.5, 6.5, 8.5, 10.5, and 24 h after starting the infusion.

The second study was performed in six rats, which were housed individually in metabolic cages and received a single 0.5-h intravenous infusion of XueBiJing at 10 ml/kg. Urine and fecal samples were collected before and 0–4, 4–8, and 8–24 h after starting the infusion and were weighed. During sampling, the sample collection tubes of the cages were frozen at −15°C.

The third study was performed in six rats that received a single 0.5-h intravenous infusion of XueBiJing at 10 ml/kg. Bile samples were collected before and 0–2, 2–4, 4–8, and 8–24 h after starting the infusion and were weighed.

The fourth study was a tissue distribution study, which was performed in 20 rats that received a single intravenous bolus dose of XueBiJing at 10 ml/kg through the tail veins. The rats were randomly assigned to four groups (five rats/group), each group corresponding to a tissue sampling time. In brief, rats under isoflurane anesthesia were killed by bleeding from the abdominal aorta at 0.08, 0.25, 0.5, and 1 h after dosing; selected tissues (the lungs, heart, brain, kidneys, and liver) were excised, rinsed in ice-cold saline, blotted, weighed, and homogenized in four-fold volumes of ice-cold saline. Rat bloods were also collected.

The fifth study was to estimate the susceptibility of senkyunolide I to influence by matrix components of XueBiJing. A total of 12 rats were randomly assigned to two groups (six rats/group) to receive a single 0.5-h intravenous infusion of XueBiJing at 10 ml/kg (each milliliter of XueBiJing containing 0.3 μmol of senkyunolide I) or the injectable solution of purified senkyunolide I at 3.0 μmol/kg. Serial blood samples (around 80 μl each time) were collected before and 0.08, 0.25, 0.5 (just before terminating the infusion), 0.58, 0.75, 1, 1.5, 2.5, 4.5, 6.5, 8.5, 10.5, and 24 h after starting the infusion.

Blood samples from the first, fourth, and fifth rat studies were heparinized and centrifuged to obtain the plasma fractions. Rat plasma, urine, and bile samples were stored at −70°C, without use of any preservative, until analysis.

Supportive In Vitro Characterizations of Phthalides.

Metabolism Studies. In vitro metabolism studies were performed to characterize tentative XueBiJing phthalide metabolites that had been detected in vivo. Because of detection of glucuronides of XueBiJing phthalides in excretory samples of human subjects and rats receiving XueBiJing, senkyunolides I, G, H, and N, and 3-hydroxy-3-*n*-butylphthalide (10 μM for each) were separately incubated with 0.5 mg protein/ml HLM or RLM, fortified with 2 mM UDP-GlcUA; the incubation conditions were as described by Hu et al. (2013). The preceding in vitro glucuronidation of senkyunolide I was repeated, but with addition of GSH (10 mM) into the incubation. In addition, senkyunolide I was incubated directly with GSH to check the occurrence of any GSH conjugates. The metabolites formed in vitro were analyzed and compared with the respective metabolites detected in vivo, in terms of accurate molecular mass, diagnostic fragment ion/neutral loss, and chromatographic retention time.

To identify which human UGT isoforms could mediate the glucuronidation of senkyunolide I, the cDNA-expressed human UGT enzymes UGT1A1, UGT1A3, UGT1A4, UGT1A6, UGT1A7, UGT1A8, UGT1A9, UGT1A10, UGT2B4, UGT2B7, UGT2B10, UGT2B15, and UGT2B17 were fortified with UDP-GlcUA and incubated with the test compound (50 μM) for 120 min. The enzymes that could mediate the glucuronidation of senkyunolide I were identified based on the formation of senkyunolide I-7-*O*-β-glucuronide.

Before comparing UGT1A9, UGT2B15, and UGT2B17, with respect to metabolic capability for mediating glucuronidation of senkyunolide I, and similarly comparing HLM and RLM, a pilot study was performed to ensure that the assessments were under linear conditions, i.e., incubation time and enzyme concentration, for senkyunolide I-7-*O*-β-glucuronide formation. Thereafter, incubations were performed in duplicates in a total assay volume of 100 μl with each sample, which included HLM (or RLM, cDNA-expressed human UGT1A9, UGT2B15, or UGT2B17; each at 0.25 mg protein/ml), senkyunolide I (1–1000 μM), UDP-GlcUA (2 mM) and alamethicin (25 μg/ml). BSA (0.5%) was also included in the incubation to sequester unsaturated long-chain fatty acids present in HLM and RLM (Rowland et al., 2007). The reactions were terminated by adding 200 μl of ice-cold methanol after 20-min incubation with cDNA-expressed UGT1A9 (or UGT2B15, or UGT2B17) or 2-min incubation with HLM (or RLM).

Assessment of Protein Binding (Total Plasma and Individual Proteins). The unbound fraction in plasma (f_u) was assessed, in triplicate, for senkyunolides I, G, H, and N, and 3-hydroxy-3-*n*-butylphthalide by a rapid ultrafiltration method (i.e., at 13,362 *g* and 37 ℃ for 3 min) by Guo et al. (2006). Human and rat plasma samples that were obtained just before terminating the infusion of XueBiJing were immediately filtered using Microcon YM-30 centrifugal filter devices (Millipore, Bedford, MA). The concentrations of the test compounds in the filtrates, as well as the total (unbound plus bound) concentrations in the pre-treated plasma samples, were measured. Nonspecific binding of the test compounds to the filter membrane was negligible. The f_u (%) was calculated using the following equation:

$$f_u = (C_u/C_t) \times 100\% \quad (1)$$

where C_u is the concentration (nM) in the filtrate after ultrafiltration and C_t is the total concentration (nM) in the pre-treated plasma. Because of extensive binding to human plasma protein, senkyunolide G was re-assessed, in triplicate, with respect to f_u by adding the compound into pre-dose blank plasma at a high concentration of 8.0 μM using the rapid ultrafiltration method. In addition, to understand the proteins responsible for the binding in human plasma, senkyunolides I and G were assessed in triplicate in solutions of isolated human plasma proteins, i.e., albumin (600 μM), α_1-acid glycoprotein (10 μM), γ-globulins (80 μM), high density lipoproteins (10 μM), low density lipoproteins (1 μM), and very low density lipoproteins (0.1 μM), using the rapid ultrafiltration method. The test concentrations of senkyunolide I were 0.3, 0.6, 1.2, and 2.4 μM, whereas those of senkyunolide G in the isolated plasma protein solutions were 1.0, 2.0, 4.0, and 8.0 μM. The total binding constant (n*K*; 1/μM) for each isolated plasma protein was calculated using the following equation:

$$nK = (C_t - C_u)/(C_u \times [P]) \quad (2)$$

where C_t is the total concentration (nM) in the isolated plasma protein solution before ultrafiltration, C_u is the concentration (nM) in the filtrate after ultrafiltration, and [P] is the protein concentration (μM) in the protein solution (Combes et al., 2000).

Caco-2 Cell-based Assessment of Membrane Permeation Rate. To help understand their in vivo reach, rates of membrane permeation of senkyunolides I, G, H, and N, and 3-hydroxy-3-*n*-butylphthalide were assessed in triplicate using Caco-2 cell monolayers under "sink" conditions (Dai et al., 2008; Li et al., 2012). Before the assessment of the test compounds, the applicability of Caco-2 cell monolayers was validated using antipyrine, atenolol, rhodamine 123, sulfasalazine, verapamil, indomethacin, and novobiocin. Concentrations of the test compounds on the donor side (collected before incubation and at 15-min incubation) and on the receiver side (collected at 15-min incubation) were measured. The apparent permeability coefficient (P_{app}; cm/s) was calculated using the following equation:

$$P_{app} = (\Delta Q/\Delta t)/(A \times C_0) \quad (3)$$

where $\Delta Q/\Delta t$ is the linear appearance rate (μmol/s) of the test compound on the receiver side, A is the surface area (cm^2) of the cell

monolayer and C_0 is the initial concentration (μM) of the test compound on the donor compartment. A bidirectional transport experiment, i.e., apical→basolateral (A-B) and basolateral→apical (B-A), was conducted and efflux ratio (EfR, calculated using $P_{app,B\text{-}A}/P_{app,A\text{-}B}$) of the test compound was used to investigate the possible involvement of transporter-mediated efflux. An EfR > 3 was considered a positive result.

Assessment of Blood-plasma Partition. Freshly collected and heparinized pre-dose blank human and rat blood samples were spiked with senkyunolides I, G, H (for rat blood only), and N (for rat blood only), and 3-hydroxy-3-*n*-butylphthalide (for rat blood only) at concentrations of 0.18 and 0.90 μM to assess, in triplicate, the compounds' blood-to-plasma concentration ratios (B/P ratio) using a method by Chen et al. (2013). In brief, after incubation at 37 ℃ for 0.08, 0.25, 0.5, and 1 h, the blood samples were centrifuged; the resulting plasma and erythrocyte fractions were analyzed to determine the concentration of the test compound. The B/P ratio was calculated using the following equation:

$$\text{B/P ratio} = [H \times C_E + (1 - H) \times C_P]/C_P \quad (4)$$

where C_E and C_P are concentrations (nM) of test compound in the erythrocytes and plasma, respectively. The measured hematocrit values (H) of human and rat blood samples were 0.40 and 0.44, respectively.

Preparation of Glucuronides of Senkyunolide I and Their Structural Elucidation by NMR. Because the in vivo and in vitro metabolism studies indicated that the major circulating phthalide senkyunolide I was primarily eliminated by glucuronidation, the two important glucuronide metabolites of senkyunolide I were synthesized by rat hepatic microsomal UGT-mediated biotransformation of senkyunolide I. In brief, isolated senkyunolide I (80 mg) was dissolved in 65 ml of distilled water and then mixed with 5 ml of 8.5 mg protein/ml RLM, 8 ml of 500 mM Tris-HCl buffer (pH 7.4), 4 ml of 200 mM $MgCl_2$ solution, 4 ml of 500 μg/ml aqueous solution of alamethicin, and 4 ml of 200 mM aqueous solution of UDP-GlcUA. After incubation for 12 h, the reaction was terminated using 270 ml of ice-cold methanol. After centrifugation at 4,863 *g* for 10 min, the supernatant was evaporated to dryness under reduced pressure at 60 ℃. The residual was reconstituted in water and separated on a Welch Materials Ultimate XB-C18 10-μm column (250 × 50 mm i.d.; Jinhua, Zhejiang Province, China). The mobile phase consisted of methanol/water (41:59, v/v; containing 1.35 mM trifluoroacetic acid) and was delivered at 50 ml/min using Shimadzu LC-20AP pumps (Kyoto, Japan). The chromatographic separation was monitored at 280 nm, and the fractions containing target compounds were collected at 24.5–26.0 and 26.2–28.2 min, respectively. After removing methanol and trifluoroacetic acid under reduced pressure, the residuals were freeze-dried.

After being dissolved in deuterated dimethyl sulfoxide, the purified compounds were analyzed by NMR spectrometry using a Bruker AVANCE III-500 MHz spectrometer (Bremen, Germany) at 25 ℃. To elucidate the chemical structures of the purified compounds, the following NMR spectra were acquired: ^{1}H NMR, ^{13}C NMR, ^{1}H-^{1}H correlated spectroscopy, ^{1}H-^{13}C heteronuclear single quantum correlation, and ^{1}H-^{13}C heteronuclear multiple bond correlation spectra.

Detection and Characterization of Unchanged and Metabolized Phthalides. A Waters Synapt G2 high definition time-of-flight mass spectrometer (Manchester, UK), interfaced via a Zspray/LockSpray electrospray ionization (ESI) source with a Waters Acquity UPLC separation module (Milford, MA), was used to analyze phthalides in samples of XueBiJing, pulverized Chuanxiong, and pulverized Danggui and to analyze unchanged and metabolized phthalides in human and rat samples. Samples from the in vitro metabolism studies were also analyzed. Samples were prepared as follows: (1) dilution with water, for the samples of XueBiJing; (2) extraction with 50% methanol and filtration, for the samples of pulverized Chuanxiong and pulverized Danggui; and (3) protein precipitation with methanol and centrifugation, for the samples of human, rat, and in vitro metabolism studies. Chromatographic separation was achieved on a Waters ACQUITY UPLC BEH C18 1.7-μm column (100 × 2.1 mm i.d.; Dublin, Ireland; maintained at 40 ℃) using a mobile phase that consisted of solvent A (water/methanol, 99:1, v/v; containing 1 mM formic acid) and solvent B (water/methanol, 1:99, v/v; containing 1 mM formic acid). The mobile phase was delivered at 0.3 ml/min in a gradient manner, i.e., 0–2 min, at 2% solvent B; 2–32 min, from 2% to 98% solvent B; 32–37 min, at 98% solvent B; and 37–42 min, at 2% solvent B. Mass spectrometry was set in the sensitivity mode with a resolving power of around 10,000. The ion source worked both in the positive or negative ion modes under the following conditions: capillary voltage at 3.0 kV (positive ion mode) or −2.5 kV (negative ion mode), source temperature of 120 ℃, desolvation gas at 850 l/h and 450 ℃, sampling cone at 40 V, and extraction cone at 4.0 V. The mass spectrometer was externally calibrated over a range of *m/z* 50–1000 using a 5 mM sodium formate solution at 20 μl/min and mass shifts during acquisition were corrected using leucine enkephalin (*m/z* 556.2771 for the positive ion mode and *m/z* 554.2615 for the negative ion mode) as a lockmass. MS^E data acquisition (in centroid mode, *m/z* 50–1000) was achieved using a trap collision energy of 4 V and a trap collision energy ramp of 20–30 V simultaneously with a scan time of 0.3 s. MS^E acquisition time was set over a retention time range of 5–37 min. Instrument control and data acquisition were achieved using Waters MassLynx software (version 4.1; Manchester, UK).

To facilitate analysis of phthalides and related compounds in samples of different types, pre-analysis literature mining was conducted on phthalides of Chuanxiong and/or Danggui origin with respect to their names, chemical structures, presence in raw materials of Chuanxiong and Danggui and in Chinese medicines containing these herbs, pharmaceutical processing-related chemotransformation, liquid chromatography/mass spectrometry-based analysis, pharmacokinetics and metabolism, antisepsis-related properties, and toxicities. Information retrieval for the literature mining was performed by constructing a template (comprising the search terms) to retrieve the related titles and abstracts of literature from the electronic databases PubMed and China National Knowledge Infrastructure. Search terms

were ‘phthalide’, ‘*Ligusticum*’, ‘*Angelica*’, ‘Chuanxiong’, and ‘Danggui’. Two reviewers independently screened all the tiles and abstracts and their disagreements in screening results were resolved by consensus. These reviewers then worked together to perform manually information extraction. In addition, detection of metabolized phthalides in samples from human and rat studies was also facilitated by Accelrys metabolite database (version 2015.1; San Diego, CA), which was used to predict possible metabolic pathways of phthalides (Williams et al., 2012).

Detection of phthalides in samples of XueBiJing and subsequent detection of unchanged and metabolized phthalides in samples from the human and rat studies were achieved using an analyte-targeted detection approach working in the positive ESI mode. The key to this approach is to generate a compound list for compounds’ detection based on their accurate molecular masses and ESI pattern(s). Generating such compound lists depended on both the types of sample and those of analyte. In this study, (1) compound list for the detection of phthalides in XueBiJing was generated from the results of analyses of pulverized samples of Chuanxiong and Danggui; this sample list, before use, was supplemented with pre-analysis information regarding pharmaceutical processing-related chemotransformation of phthalides. Compound lists for the analyses of the samples of Chuanxiong and Danggui were generated from the pre-analysis information regarding chemical composition of the herbs. (2) Compound lists for the detection of unchanged phthalides in samples from the human and rat studies were generated from the results of analysis of the dosed XueBiJing. (3) Compound lists for the detection of phases I and II metabolites of the major XueBiJing phthalides in human and rat samples were generated from pre-analysis information regarding molecular mass gains and losses for the possible metabolites compared with those of their parent compounds. In addition, two other detection approaches, i.e., background subtraction (Zhang and Yang, 2008) and searching for diagnostic fragment ions and neutral losses (Levsen et al., 2005; Ma and Chowdhury, 2011; Huang et al., 2015), were also used and served to confirm and supplement the result of analyte-targeted detection approach. To this end, the phthalides present in the pulverized samples of Chuanxiong and Danggui were also detected by the background-subtraction-based approach, which involved using proper background control samples that were prepared in parallel with the test samples of extracts, except for no herb being put into the preparation. Such confirmation and supplementary evaluation were also conducted, for detection of phase II metabolites of phthalides in human and rat samples, by the diagnostic fragment ion/neutral loss-based search approach. The diagnostic fragment ion for detection of the GSH conjugates was at *m/z* 272.0883 in the negative ESI mode, while the diagnostic neutral losses for detection of the sulfates, cysteine conjugates, GSH conjugates, *N*-acetylcysteine conjugates, glucuronides, and cysteinylglycine conjugates were 79.9568, 121.0197, 129.0426, 163.0303, 176.0321, and 178.0412 Da, respectively, in the positive ESI mode.

Characterization of the phthalides detected in XueBiJing was based on comparison with their corresponding reference standards, with respect to their ionization and fragmentation profiles and chromatographic retention times. When the reference standards were not available, characterization of major phthalides was performed after the associated reference standards were isolated and purified from pulverized Chuanxiong or Danggui and their chemical structures were elucidated by NMR spectrometry, while characterization of minor phthalides was based on comparison of their ionization, fragmentation, and chromatographic profiles with the respective reported ones, if any available, for the suspected compounds. Characterization of the detected unchanged phthalides in samples from the human and rat studies was based on comparison of their ionization, fragmentation, and chromatographic profiles with the respective profiles of characterized phthalides that were present in the sample of XueBiJing (serving as reference). Characterization of the detected phthalide metabolites was based on the in vitro metabolism study, which simulated the in vivo metabolic reactions using the associated parent compounds, drug-metabolizing enzymes, and cofactors (see preceding subsection). Important metabolites detected, including major circulating metabolites and/or products of metabolic pathways that serve as the primary routes for elimination of the parent compounds, were synthesized and purified for further characterization. After the synthesized compound and the detected metabolite were characterized as the same compound by liquid chromatography/mass spectrometry-based analysis, the chemical structure of the metabolite was then elucidated by NMR analysis of the synthesized compound (see preceding subsection). To help evaluate the importance of the detected compounds in the early stage of the study, preliminary quantification was performed by calibration with the available reference standard or, when the reference standard was not available, by calibration with another compound, of which the reference standard was available, of close structural similarity to the analyte.

Quantification of Phthalides. For accurate and relatively high throughput quantification of the major phthalides in the samples of XueBiJing and of the major circulating phthalides and the important metabolites in the human, rat, and in vitro studies, an Applied Biosystems Sciex API 4000 Q Trap mass spectrometer (Toronto, Canada), interfaced via a Turbo V ion source with a Waters Acquity UPLC separation module (Milford, MA), was used with the reference standard for calibration of each analyte. Sample preparation methods for the quantification were the same as those for the detection (see preceding subsection). Chromatographic separation was achieved on a Waters CORTECS UPLC C18 1.6-μm column (50 × 2.1 mm i.d.; Dublin, Ireland; maintained at 45 ℃) using a mobile phase, which consisted of solvent A (water/methanol, 99:1, v/v; containing 1 mM formic acid and 25 μM lithium acetate) and solvent B (water/methanol, 1:99, v/v; containing 1 mM formic acid and 25 μM lithium acetate). The mobile phase was delivered at 0.35 ml/min in a gradient manner, i.e., 0–7 min, from 6% to 82% solvent B; 7–8 min, at 6% solvent B. The instrument parameters for mass spectrometry were optimized in the positive ion mode to maximize the generation of lithium adducts for the analytes and to yield their characteristic product ions. The precursor-to-product ion pairs used for multiple-reaction-monitoring of senkyunolides I, H, G, and N,

3-hydroxy-3-*n*-butylphthalide, and senkyunolide I-7-*O*-β-glucuronide were *m/z* 231.1→202.3 (the optimized collision energy, 29 V), 231.1→184.0 (31 V), 215.0→191.0 (30 V), 233.1→171.2 (29 V), 213.0→189.0 (27 V), and 407.2→231.2 (33 V), respectively. Instrument control and data acquisition were achieved using Waters Empower 2 software (Milford, MA) and Applied Biosystems Analyst software (version 1.5.1; Foster City, CA). Matrix-matched calibration curves of senkyunolides I, H, G, and N, 3-hydroxy-3-*n*-butylphthalide, and senkyunolide I-7-*O*-β-glucuronide were constructed using weighted ($1/X$ or $1/X^2$) linear regression of the peak areas (Y) of the analytes against the corresponding nominal analytes' concentrations (X; 6, 19, 56, 167, 500, 1500, and 4500 nM), and the curves showed good linearity ($r^2 > 0.99$). No internal standard was used in the multi-analyte quantification, because it is difficult to select an appropriate internal standard for a wide variety of analytes and because introducing multiple internal standards may limit the assay performance (Niessen et al., 2006; Li et al., 2007). The assays were validated according to the European Medicines Agency Guideline on Bioanalytical Method Validation (2012; www.ema.europa.eu) to demonstrate their reliability and reproducibility for the intended use. The assays' lower limits of quantification were 19–56 nM for the analytes and the upper limits of quantification were 4500 nM. The intra-batch accuracy and precision were 86–112% and 2–15%, respectively, while the inter-batch values were 95–113% and 3–12%, respectively. The coefficients of variation of matrix factors were 1.3–13.6%, which were within the required range, i.e., ≤ 15%. The stability of analytes under conditions mimicking the analytical process was evaluated: after storage at 24 ℃ for 5 h, after storage at 8 ℃ for 24 h, and after three freeze-and-thaw cycles. The test compounds were stable under the test conditions, because the results, i.e., −15–9%, met the acceptance criterion (the measured mean concentration being within ±15% of the nominal concentration).

Data Analysis. Pharmacokinetic parameters of phthalides detected in human subjects and rats (senkyunolide I only) were estimated by non-compartmental analysis using Thermo Scientific Kinetica software package (version 5.0; Philadelphia, PA). Dose proportionality of senkyunolide I in the rats was assessed using the regression of log-transformed data (the Power model), with the criteria calculated according to a method by Smith et al. (2000). Michaelis constant (K_m) and maximum velocity (V_{max}) were determined by nonlinear regression analysis of initial rates of senkyunolide I-7-*O*-β-glucuronide formation as a function of the concentration of the substrate senkyunolide I, using GraphPad Prism software (version 5.01; San Diego, CA); in vitro intrinsic clearance (CL_{int}) was calculated from the ratio of V_{max} to K_m. Statistical analysis was undertaken using IBM SPSS Statistics software (version 19.0; Somers, NY). Data from this study were assumed to be normally distributed and comparisons between two groups were performed by means of Student's unpaired *t*-test. All data are expressed as the mean ± S.D. $P < 0.05$ was considered the minimum level of statistical significance.

References

Chen F, Li L, Xu F, Sun Y, Du F-F, Ma X-T, Zhong C-C, Li X-X, Wang F-Q, Zhang N-T, and Li C (2013) Systemic and cerebral exposure to and pharmacokinetics of flavonols and terpene lactones after dosing standardized *Ginkgo biloba* leaf extracts to rats via different routes of administration. *Br J Pharmacol* **170:** 440–457.

Combes O, Barré J, Duché J-C, Vernillet L, Archimbaud Y, Marietta MP, Marietta MP, Tillement J-P, and Urien S (2000) In vitro binding and partitionning of irinotecan (CPT-11) and its metabolite, SN-38, in human blood. *Invest New Drugs* **18:** 1–5.

Dai J-Y, Yang J-L, and Li C (2008) Transport and metabolism of flavonoids from Chinese herbal remedy Xiaochaihu-tang across human intestinal Caco-2 cell monolayers. *Acta Pharmacol Sin* **29:** 1086–1093.

Guo B, Li C, Wang G-J, and Chen L-S (2006) Rapid and direct measurement of free concentrations of highly protein-bound fluoxetine and its metabolite norfluoxetine in plasma. *Rapid Commun Mass Spectrom* **20:** 39–47.

Hu Z-Y, Yang J-L, Cheng C, Huang Y-H, Du F-F, Wang F-Q, Niu W, Xu F, Jiang R-R, Gao X-M, and Li C (2013) Combinatorial metabolism notably affects human systemic exposure to ginsenosides from orally administered extract of *Panax notoginseng* roots (Sanqi). *Drug Metab Dispos* **41:** 1457–1469.

Huang K, Huang L-Y, and van Breemen RB (2015) Detection of reactive metabolites using isotope-labeled glutathione trapping and simultaneous neutral loss and precursor ion scanning with ultra-high-pressure liquid chromatography triple quadruple mass spectrometry. *Anal Chem* **87:** 3646–3654.

Levsen K, Schiebel H-M, Behnke B, Dötzer R, Dreher W, Elend M, and Thiele H (2005) Structure elucidation of phase II metabolites by tandem mass spectrometry: an overview. *J Chromatogr A* **1067:** 55–72.

Li L, Liang S-P, Du F-F, and Li C (2007) Simultaneous quantification of multiple licorice flavonoids in rat plasma. *J Am Soc Mass Spectrom* **18:** 778–782.

Li L, Zhao Y-S, Du F-F, Yang J-L, Xu F, Niu W, Ren Y-H, and Li C (2012) Intestinal absorption and presystemic elimination of various chemical constituents present in GBE50 extract, a standardized extract of *Ginkgo biloba* leaves. *Curr Drug Metab* **13:** 494–509.

Ma S-G and Chowdhury SK (2011) Analytical strategies for assessment of human metabolites in preclinical safety testing. *Anal Chem* **83:** 5028–5036.

Niessen WMA, Manini P, and Andreoli R (2006) Matrix effects in quantitative pesticide analysis using liquid chromatography-mass spectrometry. *Mass Spectrom Rev* **25:** 881–899.

Reagan-Shaw S, Nihal M, and Ahmad N (2008) Dose translation from animal to human studies revisited. *Faseb J* **22:** 659–661.

Rowland A, Gaganis P, Elliot DJ, Mackenzie PI, Knights KM, and Miners JO (2007) Binding of inhibitory fatty acids is responsible for the enhancement of UDP-glucuronosyltransferase 2B7 activity by albumin: implications for in vitro-in vivo extrapolation. *J Pharmacol Exp Ther* **321:** 137–147.

Smith BP, Vandenhende FR, DeSante KA, Farid NA, Welch PA, Callaghan JT, and Forgue ST (2000) Confidence interval criteria for assessment of dose proportionality. *Pharm Res* **17:** 1278–1283.

Williams AJ, Ekins S, Spjuth O, and Willighagen EL (2012) Accessing, using, and creating chemical property databases for computational toxicology modeling. *Methods Mol Biol* **929:** 221–241.

Zhang H-Y and Yang Y-O (2008) An algorithm for thorough background subtraction from high-resolution LC/MS data: application for detection of glutathione-trapped reactive metabolites. *J Mass Spectrom* **43:** 1181–1190.

Zhong C-C, Chen F, Yang J-L, Li L, Cheng C, Du F-F, Jia W-W, Zhang N-T, Olaleye OE, Pintusophon S, Wang F-Q, Xu F, Zhang S-P, Xie C-Y, Lou L-G, Chen D-Y, Niu W, and Li C (2017) Pharmacokinetics and disposition of anlotinib, an oral tyrosine kinase inhibitor, in experimental animal species. *Acta Pharmacol Sin* (accepted).

Supplemental Table 1

Time schedules for blood and urine sampling in human pharmacokinetic study

Dosage Regimen 1 (1.25-h infusion, 100 ml/day)				Dosage Regimen 2 (2.5-h infusion, 100 ml/day)		Dosage Regimen 3 (1.25-h infusion, 50 ml/day)	
Time	Day 1	Days 2–6	Day 7	Time	Day 1	Time	Day 1
h				*h*		*h*	
Blood sampling							
Before infusion of XueBiJing							
0	+	+	+	0	+	0	+
After starting the infusion							
0.17	+	—	+	0.17	+	0.17	+
0.5	+	—	+	0.5	+	0.5	+
1.25	+	+	+	1.25	+	1.25	+
—	—	—	—	2.5	+	—	—
After terminating the infusion							
0.17	+	—	+	0.17	+	0.17	+
0.5	+	—	+	0.5	+	0.5	+
1	+	—	+	1	+	1	+
2	+	—	+	2	+	2	+
4	+	—	+	4	+	4	+
8	+	—	+	8	+	8	+
—	—	—	—	21.5	+	—	—
22.75	(+)	(+)	+	—	—	22.75	+
Urine sampling							
Before infusion of XueBiJing							
0	+	—	+	0	+	0	+
After starting the infusion							
0–3	+	—	+	0–3	+	0–3	+
3–6	+	—	+	3–6	+	3–6	+
6–10	+	—	+	6–10	+	6–10	+
6–24	+	—	+	6–24	+	6–24	+

+, sampling; —, no time point or no sampling.

Supplemental Table 2

Systemic exposure to and elimination of phthalides in human subjects and rats after dosing XueBiJing

The details of the human and rat pharmacokinetic studies are described in *Supplemental Materials and Methods* (Human Pharmacokinetic Study of XueBiJing and Supportive Rat Pharmacokinetic Studies of XueBiJing). The data represent mean ± S.D.

Compound	Human Subjects (n = 12)		Rats (n = 6)		
	$AUC_{0-\infty}$	$Cum.A_{e\text{-}U\ 0-24h}$	$AUC_{0-\infty}$	$Cum.A_{e\text{-}U\ 0-24h}$	$Cum.A_{e\text{-}B\ 0-24h}$
	nM·h	*nmol*	*nM·h*	*nmol*	*nmol*
Senkyunolide I (**15**)	631 ± 139	1255 ± 296	539 ± 108	5.93 ± 1.19	16.6 ± 3.3
Senkyunolide G (**12**)	1648 ± 299	—	104 ± 21	—	—
Senkyunolide H (**16**)	112 ± 27	264 ± 78	120 ± 24	1.03 ± 0.21	5.00 ± 1.00
Senkyunolide N (**17**)	105 ± 40	168 ± 64	103 ± 21	2.06 ± 0.41	—
3-Hydroxy-3-*n*-butylphthalide (**10**)	247 ± 40	424 ± 98	112 ± 22	0.75 ± 0.15	0.30 ± 0.06

$AUC_{0-\infty}$, area under concentration-time curve from 0 to infinity; $Cum.A_{e\text{-}U\ 0-24h}$, cumulative amount excreted into urine from 0 to 24 h; $Cum.A_{e\text{-}B\ 0-24h}$, cumulative amount excreted into bile from 0 to 24 h.

Supplemental Table 3

Metabolites of senkyunolide I (**15**) detected in the urine of human subjects who received a 1.25-h intravenous infusion of XueBiJing at 100 ml/subject

The details of the human pharmacokinetic study are described in *Supplemental Materials and Methods* (Human Pharmacokinetic Study of XueBiJing).

Metabolite Type	Metabolite ID[a]	LC/TOF-MS^E Data			Molecular Mass	Molecular Formula
		t_R	Ionized Molecule	Diagnostic NL		
		min	*m/z*	*Da*	*Da*	
*Parent compound: senkyunolide I (**15**)*						
Glucuronide	**M15$_{G-1}$**	12.71	$[M+Na]^+$/423.1263	176.0317	400.1369	$C_{18}H_{24}O_{10}$
	M15$_{G-2}$	13.40	$[M+Na]^+$/423.1263	176.0318		
Cysteine conjugate	**M15$_{Cys-1}$**	14.05	$[M+H]^+$/328.1217	121.0200	327.1140	$C_{15}H_{21}NO_5S$
	M15$_{Cys-2}$	14.63	$[M+H]^+$/328.1217	121.0199		

LC/TOF-MS, liquid chromatography/time-of-flight mass spectrometry; t_R, retention time; NL, neutral loss.

[a]Metabolite ID provides information regarding parent compound, metabolite type, and metabolite isomer. For instance, M15 in **M15$_{G-1}$** denotes that the compound is a metabolite of senkyunolide I (**15**). The subscript letter G denotes glucuronide and the subscript number 1 denotes the first eluted metabolite isomer. The subscript letter Cys denotes cysteine conjugate.

Supplemental Table 4

Metabolites of senkyunolides I (**15**) and G (**12**) detected in the excretory samples of rats that received a 0.5-h intravenous infusion of XueBiJing at 10 ml/kg

The details of the rat studies are described in *Supplemental Materials and Methods* (Supportive Rat Pharmacokinetic Studies of XueBiJing).

Metabolite Type	Metabolite ID[a]	Excretory Sample	LC/TOF-MS^E Data			Molecular Mass	Molecular Formula
			t_R	Ionized Molecule	Diagnostic FI or NL		
			min	*m/z*	*m/z or Da*	*Da*	
*Parent compound: senkyunolide I (**15**)*							
Glucuronide	**M15$_{G-1}$**	Rat bile	12.72	$[M+Na]^+$/423.1272	NL, 176.0324	400.1369	$C_{18}H_{24}O_{10}$
		Rat urine	12.72	$[M+Na]^+$/423.1270	NL, 176.0317		
	M15$_{G-2}$	Rat bile	13.40	$[M+Na]^+$/423.1266	NL, 176.0321		
		Rat urine	13.40	$[M+Na]^+$/423.1271	NL, 176.0318		
GSH conjugate	**M15$_{GSH-1}$**	Rat bile	14.70	$[M+H]^+$/514.1851	NL, 129.0430	513.1781	$C_{22}H_{31}N_3O_9S$
				$[M-H]^-$/512.1704	FI, 272.0885		
	M15$_{GSH-2}$	Rat bile	15.67	$[M+H]^+$/514.1858	NL, 129.0428		
				$[M-H]^-$/512.1699	FI, 272.0881		
Cysteinylglycine conjugate	**M15$_{Cys-Gly-1}$**	Rat bile	13.54	$[M+H]^+$/385.1433	NL, 178.0416	384.1355	$C_{17}H_{24}N_2O_6S$
	M15$_{Cys-Gly-2}$	Rat bile	14.29	$[M+H]^+$/385.1430	NL, 178.0412		
Cysteine conjugate	**M15$_{Cys-1}$**	Rat bile	14.05	$[M+H]^+$/328.1216	NL, 121.0201	327.1140	$C_{15}H_{21}NO_5S$
	M15$_{Cys-2}$	Rat bile	14.63	$[M+H]^+$/328.1221	NL, 121.0199		
N-acetylcysteine conjugate	**M15$_{NAC-1}$**	Rat urine	16.75	$[M+H]^+$/370.1325	NL, 163.0300	369.1246	$C_{17}H_{23}NO_6S$
	M15$_{NAC-2}$	Rat urine	17.23	$[M+H]^+$/370.1322	NL, 163.0296		
*Parent compound: senkyunolide G (**12**)*							
Glucuronide	**M12$_G$**	Rat bile	16.63	$[M+Na]^+$/407.1311	NL, 176.0318	384.1420	$C_{18}H_{24}O_9$
		Rat urine	16.63	$[M+Na]^+$/407.1320	NL, 176.0315		

LC/TOF-MS, liquid chromatography/time-of-flight mass spectrometry; t_R, retention time; FI, fragment ion; NL, neutral loss.

[a]Metabolite ID provides information regarding parent compound, metabolite type, and metabolite isomer. For instance, M15 in **M15$_{G-1}$** denotes that the compound is a metabolite of senkyunolide I (**15**). The subscript letter G denotes glucuronide and the subscript number 1 denotes the first eluted metabolite isomer. The subscript letters GSH, Cys-Gly, Cys, and NAC denote dehydrated glutathione conjugate, cysteinylglycine conjugate, cysteine conjugate, and *N*-acetylcysteine conjugate, respectively. **M12$_G$** indicates only one senkyunolide G glucuronide detected.

Supplemental Table 5

NMR data of senkyunolide I-6-*O*-β-glucuronide (**M15$_{G-1}$**) and senkyunolide I-7-*O*-β-glucuronide (**M15$_{G-2}$**)

The details of preparation and structural elucidation of the glucuronides of senkyunolide I are described in *Supplemental Materials and Methods* (Preparation of Glucuronides of Senkyunolide I and Their Structural Elucidation by NMR).

Position	Senkyunolide I-6-*O*-β-glucuronide (**M15$_{G-1}$**)		Senkyunolide I-7-*O*-β-glucuronide (**M15$_{G-2}$**)	
	^{1}H NMR [multiplicity (J in Hz)]	^{13}C NMR	^{1}H NMR [multiplicity (J in Hz)]	^{13}C NMR
	ppm	*ppm*	*ppm*	*ppm*
1	—	168.2	—	168.9
3	—	147.9	—	148.0
3a	—	153.4	—	154.9
4	2.46, m	16.8	2.47, m	16.8
5	1.84, 2.00, m	21.9	1.81, m	23.6
6	3.88, bs	77.3	4.00, bs	66.8
7	4.25, bs	60.5	4.26, bs	70.4
7a	—	125.3	—	123.5
8	5.47, t (8.0)	112.3	5.55, t (7.8)	113.5
9	2.27, m	27.5	2.28, m	27.6
10	1.47, m	21.7	1.47, m	21.7
11	0.92, t (7.3)	13.6	0.92, t (7.3)	13.7
1′	4.30, m	102.8	4.46, d (7.7)	102.5
2′	2.85, m	73.0	2.92, t (8.6)	73.3
2′-OH	4.94, bs	—	4.74, bs	—
3′	3.15, m	76.1	3.14, t (8.9)	76.2
4′	3.18, m	71.7	3.23, t (9.2)	71.8
5′	3.45, m	74.6	3.48, d (8.6)	75.1
5′-COOH	—	171.9	—	171.3

m, multiple; bs, broad singlet; t, triplet; d, double.

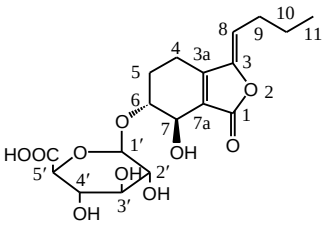

Senkyunolide I-6-*O*-β-glucuronide (**M15$_{G-1}$**)

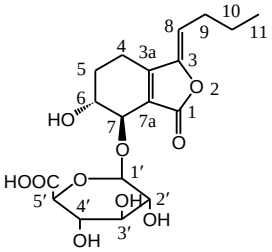

Senkyunolide I-7-*O*-β-glucuronide (**M15$_{G-2}$**)

Supplemental Table 6

Plasma and urine pharmacokinetics of senkyunolides I (**15**) and G (**12**) on day 7 in human subjects who received a 1.25-h intravenous infusion of XueBiJing at 50 ml/subject each day for seven consecutive days

The details of the human pharmacokinetic study are described in *Supplemental Materials and Methods* (Human Pharmacokinetic Study of XueBiJing). Senkyunolide G (**12**) was not detected in the urine of human subjects who received XueBiJing. The data represent mean ± S.D.

Pharmacokinetic Parameter	Senkyunolide I (**15**) (n = 6)	Senkyunolide G (**12**) (n = 6)
C_{max} (nM)	165 ± 22	240 ± 27
$AUC_{0-\infty}$ (nM·h)	293 ± 27	759 ± 119
$t_{1/2}$ (h)	0.73 ± 0.09	2.11 ± 0.56
MRT (h)	1.58 ± 0.09	3.71 ± 0.74
V_{SS} (l/kg)	1.12 ± 0.08	0.10 ± 0.01
$CL_{tot,p}$ (l/h/kg)	0.714 ± 0.070	0.027 ± 0.005
CL_R (l/h/kg)	0.024 ± 0.009	—
$f_{e\text{-}U}$ (%)	4.05 ± 1.17	—
$CL_R/(GFR \times f_u)$ ratio	0.38 ± 0.14	—
R_{ac}	1.05	0.97

C_{max}, maximum plasma concentration; $AUC_{0-\infty}$, area under concentration-time curve from 0 to infinity; MRT, mean residence time; V_{SS}, apparent volume of distribution at steady state; $CL_{tot,p}$, total plasma clearance; CL_R, renal clearance; $f_{e\text{-}U}$, fractional urinary excretion; GFR, glomerular filtration rate; f_u, unbound fraction of compound in plasma; R_{ac}, accumulation index.

Supplemental Table 7

Interspecies similarities and differences in systemic exposure to and pharmacokinetics of XueBiJing phthalides

Human	Rat	Similarity and Difference
Comparative pharmacokinetic information between human subjects and rats		
Systemic exposure to and urinary recovery of phthalides after dosing XueBiJing		
Plasma: senkyunolides I (**15**), H (**16**), G (**12**), and N (**17**), and 3-hydroxy-3-*n*-butylphthalide (**10**) detected	**Plasma:** senkyunolides I (**15**), H (**16**), G (**12**), and N (**17**), and 3-hydroxy-3-*n*-butylphthalide (**10**) detected	**Similarity:** identical XueBiJing phthalides detected in human plasma and in rat plasma; senkyunolides I (**15**) was a major circulating phthalide in human subjects and rats; identical XueBiJing phthalides detected in human urine and in rat urine
Urine: senkyunolides I (**15**), H (**16**), and N (**17**) and 3-hydroxy-3-*n*-butylphthalide (**10**) detected	**Urine:** senkyunolides I (**15**), H (**16**), and N (**17**) and 3-hydroxy-3-*n*-butylphthalide (**10**) detected	**Difference:** senkyunolides G (**12**) was a major circulating phthalide in human subjects but not in rats
*Plasma and renal pharmacokinetics of senkyunolide I (**15**)*		
$t_{1/2}$**:** 0.83 ± 0.11 h	$t_{1/2}$**:** 0.19 ± 0.03 h	**Similarity:** short $t_{1/2}$ in human subjects and in rats
V_{SS}**:** 1.26 ± 0.12 l/kg	V_{SS}**:** 2.19 ± 0.11 l/kg	**Similarity:** extensively distributed in human subjects and in rats
$CL_{tot,p}$**:** 0.747 ± 0.109 l/h/kg	$CL_{tot,p}$**:** 4.853 ± 0.545 l/h/kg	**Difference:** medium systemic clearance in human subjects, but high systemic clearance in rats
CL_R**:** 0.034 ± 0.010 l/h/kg	CL_R**:** 0.038 ± 0.012 l/h/kg	**Similarity:** renal excretion was a minor elimination route in human subjects and in rats
$f_{e\text{-}U}$**:** 4.45 ± 1.23 %	$f_{e\text{-}U}$**:** 0.67 ± 0.21 %	
$CL_R/(GFR \times f_u)$ **ratio:** 0.58 ± 0.17	$CL_R/(GFR \times f_u)$ **ratio:** 0.23 ± 0.07	**Similarity:** tubular reabsorption involved in renal excretion in human subjects and in rats
f_u**:** 53.6%	f_u**:** 48.3%	**Similarity:** not extensively bound in human plasma and in rat plasma
*Plasma and renal pharmacokinetics of senkyunolide G (**12**)*		
$t_{1/2}$**:** 2.32 ± 0.37 h	$t_{1/2}$**:** 0.15 ± 0.03 h	**Difference:** 3-times as long as $t_{1/2}$ of **15** in human subjects, but comparable to $t_{1/2}$ of **15** in rats
V_{SS}**:** 0.11 ± 0.01 l/kg	V_{SS}**:** 0.85 ± 0.10 l/kg	**Difference:** resided largely in human plasma and extracellular fluid, but extensively distributed in rats
$CL_{tot,p}$**:** 0.027 ± 0.003 l/h/kg	$CL_{tot,p}$**:** 2.536 ± 0.331 l/h/kg	**Difference:** low systemic clearance in human subjects, but medium systemic clearance in rats[a]
$f_{e\text{-}U}$**:** 0%	$f_{e\text{-}U}$**:** 0%	**Similarity:** renal excretion not important in human subjects or in rats
f_u**:** 3.0%	f_u**:** 13.3%	**Difference:** extensively bound in human plasma, but not extensively bound in rat plasma[b]
*In vivo metabolism of senkyunolide I (**15**)*		
Plasma: no metabolite detected	**Plasma:** no metabolite detected	**Similarity:** no plasma metabolite detected in human subjects or in rats
Urine: the glucuronides $\mathbf{M15_{G\text{-}1}}$ and $\mathbf{M15_{G\text{-}2}}$ and the cysteine conjugates $\mathbf{M15_{Cys\text{-}1}}$ and $\mathbf{M15_{Cys\text{-}2}}$	**Urine:** the glucuronides $\mathbf{M15_{G\text{-}1}}$ and $\mathbf{M15_{G\text{-}2}}$ and the *N*-acetylcysteine conjugates $\mathbf{M15_{NAC\text{-}1}}$ and $\mathbf{M15_{NAC\text{-}2}}$	**Similarity:** identical urinary glucuronides detected in human subjects and in rats **Difference:** other conjugates detected in the two species
*In vivo metabolism of senkyunolide G (**12**)*		
Plasma: no metabolite detected	**Plasma:** no metabolite detected	**Similarity:** no plasma metabolite detected in human subjects or in rats
Urine: no metabolite detected	**Urine:** the glucuronide $\mathbf{M12_G}$	**Difference:** no urinary metabolite detected in human subjects, but a urinary glucuronide detected in rats
*In vitro metabolism of senkyunolide I (**15**)*		
Glucuronidation: formation of $\mathbf{M15_{G\text{-}2}}$ and $\mathbf{M15_{G\text{-}1}}$ at a ratio of 66:1 after incubation of **15** with UDP-GlcUA-fortified HLM; K_m, 35 ± 3 μM V_{max}, 7360 ± 254 pmol/min/mg protein CL_{int}, 212 μl/min/mg protein	**Glucuronidation:** formation of $\mathbf{M15_{G\text{-}2}}$ and $\mathbf{M15_{G\text{-}1}}$ at a ratio of 5:1 after incubation of **15** with UDP-GlcUA-fortified RLM K_m, 185 ± 5 μM V_{max}, 12305 ± 122 pmol/min/mg protein CL_{int}, 67 μl/min/mg protein	**Similarity:** both human hepatic UGT and rat hepatic UGT mediate glucuronidation of **15** into $\mathbf{M15_{G\text{-}1}}$ and $\mathbf{M15_{G\text{-}2}}$ **Difference:** $\mathbf{M15_{G\text{-}2}}$-to-$\mathbf{M15_{G\text{-}1}}$ ratio by human UGT greater than that by rat UGT
*In vitro metabolism of senkyunolide G (**12**)*		
Glucuronidation: formation of $\mathbf{M12_G}$ after incubation of **12** with UDP-GlcUA-fortified HLM	**Glucuronidation:** formation of $\mathbf{M12_G}$ after incubation of **12** with UDP-GlcUA-fortified RLM	**Similarity:** both human hepatic UGT and rat hepatic UGT mediated glucuronidation of **12** into $\mathbf{M12_G}$ **Difference:** rate of $\mathbf{M12_G}$ formation mediated by rat UGT faster than that by human UGT
Additional pharmacokinetic information of senkyunolide I (15) obtained from the supportive rat studies		
—	**Dose proportionality:** plasma C_{max} and $AUC_{0-\infty}$ of **15** increasing as the dose of XueBiJing increased from 10 ml/kg to 90 ml/kg in a proportional manner	
—	**Biliary excretion: 15** with $f_{e\text{-}B}$ of 2.5%	
—	**Tissue distribution: 15** distributed extensively into rat lungs, heart, brain, kidneys, and liver	
—	**Pharmacokinetic matrix effects:** other compounds in XueBiJing had limited influence on plasma pharmacokinetics of **15**	

V_{SS}, apparent volume of distribution at steady state; $CL_{tot,p}$, total plasma clearance; CL_R, renal clearance; $f_{e\text{-}U}$, fraction of dose excreted into urine; GFR, glomerular filtration rate; f_u, unbound fraction of compound in plasma; HLM, human liver microsomes; RLM, rat liver microsomes; K_m, Michaelis constant;

V_{max}, maximum velocity; CL_{int}, intrinsic clearance; UGT, uridine 5′-diphosphoglucuronosyltransferase; C_{max}, maximum plasma concentration; $AUC_{0-\infty}$, area under concentration-time curve from 0 to infinity; $f_{e\text{-}B}$, fraction of dose excreted into bile. Metabolite ID provides information regarding parent compound, metabolite type, and metabolite isomer. For instance, M15 in **M15$_{G\text{-}1}$** denotes that the compound is a metabolite of senkyunolide I (**15**). The subscript letter G denotes glucuronide and the subscript number 1 denotes the first eluted metabolite isomer. The subscript letters Cys and NAC denote cysteine conjugate and *N*-acetylcysteine conjugate, respectively. **M12$_G$** indicates only one senkyunolide G glucuronide detected.

[a]Possible reasons for the interspecies difference in $CL_{tot,p}$ include differences in glucuronidation, which was significantly slower when mediated by human hepatic UGT than by rat hepatic UGT, and plasma protein binding, which was siginificantly higher in human than in rats.

[b]Possible reasons for the interspecies difference in f_u include differences between the compound's affinity for human albumin and that for rat albumin and between its extent of binding to human albumin and that to rat albumin, since human albumin shares only about 70% amino acid sequence homology with rat albumin, and albumin concentration in human plasma is higher than that in rat plasma (Peters, 1996; Zeitlinger et al., 2011).

References

Peters T (1996) *All About Albumin: Biochemistry, Genetics, and Medical Applications*, Academic Press, California.

Zeitlinger MA, Derendorf H, Mouton JW, Cars O, Craig WA, Andes D, and Theuretzbacher U (2011) Protein binding: do we ever learn? *Antimicrob Agents Chemother* **55:** 3067–3074.

Supplemental Table 8

Comparative plasma pharmacokinetics of senkyunolide I (**15**) in rats that received a 0.5-h intravenous infusion of an injectable solution of purified senkyunolide I at 3.0 μmol/kg or XueBiJing at 10 ml/kg (each milliliter of XueBiJing containing 0.3 μmol of **15**)

The details of the rat pharmacokinetic study are described in *Supplemental Materials and Methods* (Supportive Rat Pharmacokinetic Studies of XueBiJing). The data represent mean ± S.D.

Pharmacokinetic Parameter	Purified Senkyunolide I (n = 6)	XueBiJing (n = 6)
C_{max} (nM)	1061 ± 90	1060 ± 77
$AUC_{0-\infty}$ (nM·h)	629 ± 67	600 ± 60
$t_{1/2}$ (h)	0.22 ± 0.02	0.17 ± 0.01*
MRT (h)	0.49 ± 0.02	0.43 ± 0.02*
V_{SS} (l/kg)	2.09 ± 0.22	1.95 ± 0.18
$CL_{tot,p}$ (l/h/kg)	4.34 ± 0.42	4.55 ± 0.44

C_{max}, maximum plasma concentration; $AUC_{0-\infty}$, area under concentration-time curve from 0 to infinity; MRT, mean residence time; V_{SS}, apparent volume of distribution at steady state; $CL_{tot,p}$, total plasma clearance.

*P < 0.05, significantly different from the values in rats that received an injectable solution of purified senkyunolide I.

Supplemental Table 9

Pharmacokinetic markers of Chinese herbal medicines

Pharmacokinetic markers of Chinese herbal medicines (Lu et al., 2008; Hu et al., 2013; Li, 2017)

Chinese herbal medicines are often complex in chemical composition and contain multiple bioactive constituents; the effectiveness and safety of an herbal medicine normally is governed by human body exposure to its bioactive constituents and/or their bioactive metabolites. Current pharmacokinetic research on Chinese herbal medicines reveals pharmacokinetic characteristics of their bioactive constituents, including the systemic exposure and metabolism, after dosing the medicines. Such findings should be applied to guide rational clinical use of Chinese herbal medicines and to support clinical research on drug therapies including Chinese herbal medicines. To this end, a class of xenobiotic markers was proposed for use and research of complex Chinese herbal medicines (Lu et al., 2008); because the markers' identification results from pharmacokinetic research, they are referred to as pharmacokinetic markers. Pharmacokinetic markers of a Chinese herbal medicine comprise herbal compounds, unchanged and/or metabolized, that are measurable by contemporary techniques and that can reflect human body exposure to the herbal compounds responsible for or potentially related to the medicine's therapeutic action and the associated influencing factors. The usefulness of such markers identified from pharmacokinetic investigations could be expanded: here, pharmacokinetic markers are proposed to be potentially useful for reflecting abnormal cellular processes in patients receiving Chinese herbal medicine-included treatment and for predicting the prognosis in the patients.

Plasma and urinary tanshinol: pharmacokinetic markers of cardiotonic pills to reflect human body exposure to bioactive constituents originating from the pills' component herb Salvia miltiorrhiza *roots (Danshen) (Lu et al., 2008)*

Cardiotonic pills (compound Danshen droplet pills), an oral botanical drug product prepared from Danshen, *Panax notoginseng* roots (Sanqi), and *Borneolum* (Bingpian), is approved by China FDA for the treatment of stable angina pectoris. Cell- and isolated tissue-based studies have shown that Danshen catechols exhibited vasodilating, endothelial protective, cardioprotective, antithrombotic, antioxidant, and anti-inflammatory properties. Major Danshen catechols present in cardiotonic pills are tanshinol, protocatechuic aldehyde, salvianolic acids A, B, and D, rosmarinic acid, and lithospermic acid. Pharmacokinetic studies of cardiotonic pills in human subjects and dogs revealed tanshinol as the only Danshen catechol exhibiting significant and dose-dependent levels of systemic exposure and renal excretion after orally dosing the pills. Such levels of the other Danshen catechols were low due to extensive presystemic metabolism (for protocatechuic aldehyde) or poor intestinal absorption (for salvianolic acids A, B, and D, rosmarinic acid, and lithospermic acid).

*Plasma ginsenosides and 20(*S*)-protopanaxadiol and 20(*S*)-protopanaxatriol: pharmacokinetic markers of oral extract of* Panax notoginseng *roots (Sanqi) to reflect human body exposure to the herb's bioactive constituents and their metabolites (Hu et al., 2013)*

Sanqi is a medicinal herb that is listed in the Chinese Pharmacopeia. Ginsenosides are bioactive constituents of Sanqi and are believed to be responsible for the herb's therapeutic action. Sanqi ginsenosides can be classified based on their aglycones attached as 20(*S*)-protopanaxadiol-type (ppd-type) and 20(*S*)-protopanaxatriol-type (ppt-type). After oral administration of Sanqi extract, healthy human subjects were found to be exposed to unchanged and metabolized ginsenosides. The unchanged ginsenosides detected in plasma were four ppd-type ginsenosides (ginsenosides Ra_3, Rb_1, Rd, and F_2) and two ppt-type ginsenosides (ginsenoside Rg_1 and notoginsenoside R_1) with exposure levels changing in a Sanqi dose-dependent manner. Despite this detection, ginsenosides are largely unabsorbed due to their poor membrane permeability. The unabsorbed Sanqi ginsenosides were metabolized via a joint action of the colonic microflora and the host enterohepatic drug metabolizing enzymes, and the resulting metabolites detected in plasma were deglycosylated products, such as 20(*S*)-protopanaxadiol from the ppd-type ginsenosides and 20(*S*)-protopanaxatriol from the ppt-type ginsenosides and their further oxidized metabolites, i.e., **M16**, **M17**, and **M19**–**M22** from the ppd-type ginsenosides and **M4**–**M8** and **M10**–**M15** from the ppt-type ginsenosides. Despite being significantly higher than exposure levels of the respective unchanged ginsenosides, levels of systemic exposure to these metabolites changed in a Sanqi dose-independent manner and exhibited substantial interindividual differences. Notably, plasma 20(*S*)-protopanaxadiol and 20(*S*)-protopanaxatriol were found to be useful as pharmacokinetic markers to reflect the timely changes and interindividual variations in plasma levels of their respective oxidized metabolites and to reflect interindividual variations in deglycosylation activities of colonic microflora.

References

Hu Z-Y, Yang J-L, Cheng C, Huang Y-H, Du F-F, Wang F-Q, Niu W, Xu F, Jiang R-R, Gao X-M, and Li C (2013) Combinatorial metabolism notably affects human systemic exposure to ginsenosides from orally administered extract of *Panax notoginseng* roots (Sanqi). *Drug Metab Dispos* **41:** 1457–1469.

Li C (2017) Multi-compound pharmacokinetic research on Chinese herbal medicines: approach and methodology. *China J Chin Materia Medica* **42:** 607–617.

Lu T, Yang J-L, Gao X-M, Chen P, Du F-F, Sun Y, Wang F-Q, Xu F, Shang H-C, Huang Y-H, Wang Y, Wan R-Z, Liu C-X, Zhang B-L, and Li C (2008) Plasma and urinary tanshinol from *Salvia miltiorrhiza* (Danshen) can be used as pharmacokinetic markers for cardiotonic pills, a cardiovascular herbal medicine. *Drug Metab Dispos* **36:** 1578–1586.